Photovoltaic power generation modeling

Hannu-Pekka Hellman

September 22, 2011

Abstract

The purpose of this work was to produce a model that can estimate the hourly produced energy from a solar power system in real weather conditions in southern Finland. The power generation of a solar module is affected not only by the technical parameters of the module but also by the climatological conditions e.g. clearness of atmosphere and clouds. To be able to construct this kind of model, actual solar irradiation and sunshine hour data was needed to see how the cloudiness affects the irradiation. With these data a regression analysis was performed to get a equation that could estimate the solar irradiation in different times of day with different sunshine hour values.

Temperature data of southern Finland was obtained and used with the irradiation model to obtain an estimation of solar power produced from a simple solar module power equation. The probabilities of different sunshine hour values for different months, and an average value of sunshine hour for every month is calculated. With these values three different cases of power generation are constructed: one with full sunshine, one with no sunshine and one with the average value of sunshine hour. To make it easy to estimate the solar energy of different hours around the year, these three cases for three different solar module tilt angles, 0°, 42° and 90°, are calculated and monthly average values for different hours are presented in tables.

The solar irradiance model produced from the measured data is quite good and makes it easy to try to estimate the solar module power. This work does not have any actual measurement data of a solar module so the final results can not be verified. It is also acknowledged that especially the sunrise and sunset hours are problematic to model because of the horizon clearness and the transmittance properties of solar modules for greater angles of incidence. Because of these the obtained model most likely produces too optimistic values of year energies.

Contents

Symbols

G	Irradiance
H	Irradition
m	Air mass
N	Day number
P	Power
p	Air pressure
T_{a}	Ambient temperature
T_{c}	Cell temperature
T_{L}	Linke turbidity factor
t_{ssh}	Sunshine hour
α_{s}	Solar elevation angle
β	Tilt angle
β_{P}	Temperature coefficient of P_{max}
γ	Azimuth angle
δ	Declination angle
δ_{R}	Rayleigh optical thickness
η	Efficiency
θ_{i}	Angle of incidence
ϕ	Latitude
ω	Hour angle

Subscripts

b	Direct
d	Diffuse
r	Reflected
on	Extraterrestial normal
h	Hour
m	Month
H	Horizontal
T	Tilted

1 Introduction

For the last decade the climate change and the carbon dioxide emissions of power plants have been an increasing concern globally. Renewable energy sources that have no CO_2 emissions have been in the focus of both political and technological interest. The fast growing renewable energy sources, solar and wind energy, are probably the most studied and might have great potential as the technology develops. On the other hand these technologies have also significant problems as they generate electricity only when the wind blows or the Sun shines but electricity is needed round the clock and at increasing rate. This has led to the question, how much electricity it is possible to obtain from a solar module on different times of day during the year in real operating conditions.

A solar module has always a rated power value in its nameplate but it might come as a surprise that a solar module will not produce that high power rates, at least not many hours a day even in optimal locations. The angle at which the Sun radiation hits the module depends on the elevation of the Sun and the tilt angle of the module. An another very significant variable is the clouds in the sky. The probabilities of clouds or sunshine hours vary monthly during a year and they have an impact on the power generated from a solar module. With these information, a model to estimate the hourly energy obtained from solar modules is tried to be constructed.

The objective of this work is to produce a simple hourly power generation model for a solar module in southern Finland area. First the theoretical clear sky model for solar irradiance and a simple equation to estimate the power produced by a crystalline silicon solar module are presented. Then with the theoretical model and the measured irradiation data, a regression model for solar irradiation is calculated and three different cases of power production are calculated. Finally, the reliability of the regression model is evaluated and further improvements are discussed.

2 Basics

2.1 Photovoltaics

Solar energy can be converted into electricity by using photovoltaic devices such as solar modules. These modules consist of solar cells that are made of semiconductor p-n junctions that are able to produce electricity when absorbing the energy of the photons. Most of the solar cells on the market are made of single crystalline or polycrystalline silicon. Silicon is a widely used semiconductor material and it forms p-n junctions when it is doped with impurities. The layers of solar cells from top to bottom are the antireflective layer, the n-type layer, the p-type layer and the metal conductor. The photons of solar radiation travel through till p-type layer and then release electrons so a direct current will be flown. [1]

2.2 The position of the Sun and solar radiation

Solar radiation that comes to the surface of the Earth is naturally very dependent on the position of the Sun relative to the observer. To be able to estimate the available solar energy, mathematical models for the position of the Sun must be known. These equations are easy to use and quite exact. When the angle between the surface and the Sun is known, it must be decided which of the available solar radiation models is to be used. Different models estimate the attenuation of the solar radiation in the atmosphere differently and their complexity varies greatly. The model can also be formed from measured irradiance data.

The Sun radiates to all directions and its magnitude per area in the distance of 1 AU (*astronomical unit*, an average distance of the Sun and Earth) is called solar constant G_{sc}. The solar constant is 1367 W/m^2 and because of the slightly elliptic orbit of the Earth, the solar radiation perpendicular to the Sun in the upper atmosphere (extraterrestial radiation) varies with equation

$$G_{\text{on}} = G_{\text{sc}}(1 + 0.033\cos(\frac{360N}{365})), \tag{1}$$

where N is the number of the day [2, p. 9].

When calculating the position of the Sun, instead of standard local time a so called solar time is used. Solar time is defined in a way that when the Sun is at its highest point above the observer, the solar time is then noon. When this solar time is used in equations it is converted to hour angles ω. Time of one hour in hour angles is 15° while the noon is 0°. Hour angles are negative before noon and positive after. The difference between solar time and standard local time in minutes can be calculated from

$$\text{Solar time} - \text{Standard time} = 4(L_{\text{st}} - L_{\text{loc}}) + E, \tag{2}$$

where L_{st} is the meridian of the local time zone and L_{loc} is the longitude of the observer. Both of these are in degrees from the prime meridian to the west. E in the previous equation is

$$\begin{aligned} E = 229.2(&0.000075 + 0.001868\cos B - 0.032077\sin B \\ &-0.014615\cos 2B - 0.04089\sin 2B), \end{aligned} \tag{3}$$

where

$$B = (N-1)\frac{360}{365}. \tag{4}$$

[2, pp. 11-13]

The declination angle of the Sun is an another important value that must be calculated. Declination angle is the angle between the Sun and the equator of the Earth. The axis tilt of the Earth is constant 23.45° to ecliptic plane, and for different days the declination angle is calculated from

$$\delta = 23.45\sin(360\frac{284+N}{365}), \tag{5}$$

[1, p. 907]. Solar elevation angle from the horizon can now be calculated with

$$\alpha_{\text{s}} = \arcsin(\sin\phi\sin\delta + \cos\phi\cos\delta\cos\omega), \tag{6}$$

where ϕ is the latitude of the observer which is positive to north and negative to south. The azimuth of the Sun from the south in degrees is

$$\gamma_{\text{s}} = sign(\omega)\left|\arccos(\frac{\sin\alpha_{\text{s}}\sin\phi - \sin\delta}{\cos\alpha_{\text{s}}\cos\phi})\right|, \tag{7}$$

which is positive to the west. With these equations mentioned before, the angle of incidence from the normal can be calculated with

$$\theta_{\text{i}} = \arccos(\sin\alpha_{\text{s}}\cos\beta + \cos\alpha_{\text{s}}\sin\beta\cos(\gamma_{\text{s}} - \gamma)), \tag{8}$$

where β is the tilt angle of the panel from the surface of the ground and γ the azimuth of the panel from the south. [2, pp. 15-16]

The solar radiation on the surface of the Earth consists from direct, diffuse and reflected radiation. Direct radiation, also known as beam radiation, is the radiation component that comes straight from the Sun. On clear sky days almost all radiation on surface is direct but on overcast days its proportion is small or none. On this kind of cloudy days most of the radiation is diffuse radiation. Diffuse radiation scatters from the atmosphere because of different kind of particles for example water vapour and it can come to the surface indirectly from the Sun. Also when the panel is tilted, it can get reflected radiation from the ground, trees, houses, and etc. This component is usually quite small but for example snow is quite a good reflector so it might have some significance. [1, p. 913]

A clear sky model for global irradiance by Rigollier [4] et al. is used in this work. The model separates both direct and diffuse radiation models and by summing them global radiation is determined when reflective component is omitted. The direct component for irradiation on tilted surface can be calculated from

$$G_{\mathrm{b}} = G_{\mathrm{on}} \cos\theta_{\mathrm{i}} \exp(-0.8662 T_{\mathrm{L}} m \delta_{\mathrm{R}}), \tag{9}$$

where T_{L} is the Linke turbidity factor in air mass equal to 2, m is the relative optical air mass and δ_{R} is the integral Rayleigh optical thickness [4]. The relative optical air mass is defined

$$m = \frac{p/p_0}{\sin\alpha_s^{\mathrm{true}} + 0.50572(\alpha_s^{\mathrm{true}} + 6.07995)^{-1.6364}}. \tag{10}$$

The variables are calculated:

$$p/p_0 = \exp(-z/z_{\mathrm{h}}), \tag{11}$$

where z is the height above sea level in metres and the z_{h} is 8434.5 m.

$$\alpha_{\mathrm{s}}^{\mathrm{true}} = \alpha_{\mathrm{s}} + \Delta\alpha_{\mathrm{refr}}, \tag{12}$$

where

$$\Delta\alpha_{\mathrm{refr}} = 0.061359(180/\pi) \times \frac{0.1594 + 1.123(\pi/180)\alpha_{\mathrm{s}} + 0.065656(\pi/180)^2\alpha_{\mathrm{s}}^2}{1 + 28.9344(\pi/180)\alpha_{\mathrm{s}} + 277.3971(\pi/180)^2\alpha_{\mathrm{s}}^2}. \tag{13}$$

When $m \leq 20$ the Rayleigh optical thickness is estimated from equation

$$\delta_{\mathrm{R}} = \frac{1}{6.6296 + 1.7513m - 0.1202m^2 + 0.0065m^3 - 0.00013m^4} \tag{14}$$

and otherwise

$$\delta_{\mathrm{R}} = \frac{1}{10.4 + 0.718m}. \tag{15}$$

The Linke turbidity factor represents the particles in atmosphere that lower the transmittance of solar radiation. The Linke turbidity factor in an air mass equal to 2 can not be easily calculated. If the sky would be complete clear from any particles, the value of T_{L} would be 1, but in reality, a proper value for European countries is approximately 2.5 in clear winter days and 3 in summer. An estimate value for each month obtained from SoDa turbidity maps [5] will be used in this work.

The diffuse component is calculated from equation

$$G_{\mathrm{d}} = G_{\mathrm{on}} T_{\mathrm{rd}} F_{\mathrm{d}} \frac{1 + \cos\beta}{2}, \tag{16}$$

where diffuse transmission function at zenith is

$$T_{\mathrm{rd}} = -0.015843 + 0.030543T_{\mathrm{L}} + 0.0003797T_{\mathrm{L}}^2 \tag{17}$$

and a diffuse angular function is

$$F_{\mathrm{d}} = A_0 + A_1 \sin\alpha_{\mathrm{s}} + A_2 \sin^2\alpha_{\mathrm{s}}. \tag{18}$$

The coefficients A_0, A_1 and A_2 are

$$A_0 = 0.26463 - 0.061581T_{\mathrm{L}} + 0.0031408T_{\mathrm{L}}^2, \tag{19}$$

$$A_1 = 2.0402 + 0.018945T_{\mathrm{L}} - 0.011161T_{\mathrm{L}}^2, \tag{20}$$

and

$$A_2 = 1.3025 + 0.039231T_{\mathrm{L}} + 0.0085079T_{\mathrm{L}}^2, \tag{21}$$

unless the product of A_0 and T_{rd} is less than 0.002, then

$$A_0 = \frac{0.002}{T_{\mathrm{rd}}}. \tag{22}$$

[4]

The third component is the reflected irradiance which is possible to obtain when the surface is in tilted position. The amount of radiation that is obtained through reflection is quite small and very difficult to estimate so there are no very accurate models. One estimation for reflected irradiance is

$$G_{\mathrm{r}} = \rho G_{\mathrm{glob}} \frac{1 - \cos\beta}{2}, \tag{23}$$

where ρ is the reflectivity of the ground. [1, p. 931] The reflected radiation is not used in this work.

With these equations, a clear sky estimation for global irradiance can be obtained by adding the components together

$$G_{\mathrm{glob}} = G_{\mathrm{b}} + G_{\mathrm{d}} + G_{\mathrm{r}}. \tag{24}$$

2.3 Power generation model

This section presents a simple model to estimate electricity production of single and polycrystalline silicon photovoltaic systems. These crystalline silicon modules are by far the most used photovoltaic systems in large scale and they can be modeled quite easily in relatively good precision. It is assumed in this work that the solar modules work under maximum power point (MPP) which is usually the case when they are connected to an inverter. The inverter efficiency can be modeled by multiplying the power e.g. by 0.95.

The solar module manufacturers provide test results from STC (Standard Test Conditions) and also some other useful information in their data sheets. STC tests are done in 1000 W/m^2 irradiance, air mass 1.5 and with cell temperature of 25 °C. The maximum power of the solar module that is given in data sheet is the power reached in STC. As can be noticed the STC is not very realistic because the cell temperature is not this low in normal operating conditions. Therefore manufacturers also provide NOCT (Normal Operating Cell Temperature) values for modules that are tested in irradiance of 800 W/m^2, AM (air mass) 1.5 and with wind speed of 1 m/s. The normal operating temperature obtained from this test is useful when estimating the real power output of crystalline silicon module. In addition to these values,

manufacturers usually provide thermal characteristics of modules and in this model the power coefficient is needed.

In this model typical parameters for silicon cells are used. Many solar module data sheets give NOCT values approximately 45-48 °C so $T_{\mathrm{NOCT}} = 47$ °C is used in this model. Power temperature coefficient β_{P} is typically around 0.45–0.48 %/°C and here 0.45 %/°C is used.

The efficiency of the solar cell is dependent on the temperature of solar cell. Solar cells are semiconductors so they are more efficient when their temperatures are low but during sunshine their dark surface makes them quite hot compared to ambient temperature. Cell temperature is also cooled down by wind but it is omitted from this equation which is for mounted modules that can have airflow under the module. So the approximated cell temperature is linear to solar radiation with equation

$$T_{\mathrm{c}} = T_{\mathrm{a}} + (T_{\mathrm{NOCT}} - 20^{\circ}\mathrm{C})\frac{G}{800\mathrm{W/m}^2}, \tag{25}$$

where T_{a} is the ambient temperature and G the global irradiance [3]. The cell temperatures of the modules that are installed in a way the airflow can not cool down the back of the module, are significantly higher [1, p. 951]. This must be noted when estimating the cell temperature.

The efficiency of the solar module can then be estimated by different methods and one of them is

$$\eta = \eta_{\mathrm{STC}}(1 - \beta_{\mathrm{P}}(T_{\mathrm{c}} - T_{\mathrm{STC}}) + \gamma \log G), \tag{26}$$

where η_{STC} is the efficiency in STC. Mattei et al. [3] say the equation is mostly used with γ=0. Because the most known parameter of a solar module is the power instead of the efficiency, the equation can be changed to give the power

$$P = \frac{G}{1000\mathrm{W/m}^2} P_{\mathrm{max}}(1 - \beta_{\mathrm{P}}(T_{\mathrm{c}} - T_{\mathrm{STC}})), \tag{27}$$

where P_{max} is the nominal power of the module in STC. [3] This equation can also be modified to be more accurate by multiplying with inverter efficiency and relative transmittance coefficient for beam irrandiance due to reflection of the module surface. When the angle of incidence is less than 80 °, the

relative transmittance for direct radiation component can be calculated from equation

$$\mathrm{FT_b} = 1 - 0.07(\frac{1}{\cos\theta_\mathrm{i}} - 1). \tag{28}$$

For isotropic diffuse radiation a value of $\mathrm{FT_d}$=0.9 can be used. [1, p. 934] Now the final power equation would be

$$P = \frac{\mathrm{FT_b}G_\mathrm{b} + \mathrm{FT_d}G_\mathrm{d}}{1000\mathrm{W/m^2}}\eta_\mathrm{inv}P_\mathrm{max}(1 - \beta_\mathrm{P}(T_\mathrm{c} - T_\mathrm{STC})), \tag{29}$$

where η_inv is the efficiency of the inverter. In this work the relative transmittance coefficients are not used.

3 Observation data and the model

Large amounts of weather and irradiation data of Helsinki-Vantaa airport (60° 19' N, 24° 57' E, 53 m above sea level) was obtained from Finnish Meteorological Institution (FMI) [6]. Observations of global and diffuse solar irradiation, sunshine hours, cloudiness and temperature were mostly hourly and measured between 1.1.1981–10.7.2011. First the data was handled so the timestamps would be correct. The times were UTC-time so they were changed to the local standard time of Finland. This amount of data also has some error measurements or missing datapoints so those were marked so they could be noticed easily. In some data if only one value was missing somewhere it was replaced with either previous data value or with the average value of the previous and the next observation.

3.1 The regression model of global irradiation

The theoretical solar irradiance model for a horizontal plane was done with MATLAB as presented in section 2.2. Without better knowledge of the Linke turbidity values of different months, they were obtained from The SoDa service which is maintained by Armines / MINES ParisTech, Centre Energétique et Procédés (CEP) [5]. These values for the coordinates of Helsinki-Vantaa airport are presented in Table 1. These monthly average values raise a difficulty because as discrete values they cause relatively great leaps when the

Table 1: Linke turbidity values for air mass 2 in Helsinki-Vantaa airport.

January	3
February	2
March	2.35
April	2.7
May	2.7
June	2.9
July	3
August	3.3
September	3.3
October	2.9
November	2.8
December	2

Table 2: Linke turbidity factor polynomial coefficients.

a_0	a_1	a_2	a_3	a_4	a_5	a_6	a_7	a_8	a_9
2.37	14.17	-98.10	249.42	-320.85	235.94	-103.50	26.80	-3.78	0.22

month changes. To overcome this problem, a polynomial fitting is done to make values more continuous. A ninth degree polynomial fitting is done when the monthly average values are considered to be the values of the 15th day of each month and the values of the first and the last day of year should be 2.5. The day variable is divided by 100 so day number 1 is 0.01 in the equation. The equation is then in a form that the a_0 is the constant term and the a_9 is the ninth degree term. The coefficients of the polynome are in Table 2.

With theoretical global irradiance model, data of global irradiation and sunshine hours, a regression analysis was performed to obtain a model to estimate hourly solar irradiation. It should be noted that the theoretical irradiance model gives instantenous values of irradiance G (W/m^2) as the irradiation data has measured the energy H (Wh/m^2) of one hour. The values are quite at the same level but it is probably not the most precise method. To estimate the irradiation of next hour, these all data were imported to MATLAB and the following regression model was decided to be used:

$$H_{fit} = \beta_0 + \beta_1 G_{\mathrm{glob}} + \beta_2 t_{\mathrm{ssh}} + \beta_3 G_{\mathrm{glob}} t_{\mathrm{ssh}} + \beta_4 G_{\mathrm{glob}}^2 + \beta_5 t_{\mathrm{ssh}}^2. \qquad (30)$$

Table 3: Global irradiation coefficients for a horizontal plane.

n	0	1	2	3	4	5
β_{n}	0.123	0.335	120.55	0.641	-6.2×10^{-5}	-102.35
s.e.	0.161	0.002	1.835	0.0018	2.98×10^{-6}	1.915
z-score β_{n}	111.325	80.686	43.988	115.469	-10.144	-35.395
s.e.	0.122	0.478	0.670	0.319	0.490	0.662
p-value	44.5 %	0 %	0 %	0 %	0 %	0 %

In equation 30, β_{n}, n=0, 1, 2, 3, 4, 5 are the regression coefficients, G_{glob} is the theoretical irradiance value and t_{ssh} is the sunshine hour value between 0–1. With irradiation data of a 01.01.2000–31.12.2009 for horizontal surface and 01.01.2000–31.12.2007 for 42° and 90° tilted surfaces, these regression coefficients were obtained and used to estimate the global irradiation in southern Finland area. The shorter observation data used for the tilted model is because of few months of missing diffuse radiation data in 2008. The leap days are inserted to the theoretical clear sky global irradiance model in such a way that the 29th day of February has the same theoretical values as the 28th day. In the case of a tilted surface, a little different method had to be used because the irradiation data is for horizontal surface. The direct irradiation on horizontal surface was obtained by subtracting the measured diffuse irradiation from the global irradiation. If the direct irradiation was negative, it was changed to zero. Then the horizontal direct and diffuse irradiation components were changed for the tilted surface with the following equations

$$H_{\mathrm{b,T}} = H_{\mathrm{b,H}} \frac{\cos\theta_{\mathrm{i}}}{\sin\alpha_{\mathrm{s}}}, \tag{31}$$

and

$$H_{\mathrm{d,T}} = H_{\mathrm{d,H}} \frac{1+\cos\beta}{2}, \tag{32}$$

and added together [2, p. 90]. In the case of tilted surface, the direct irradiation was only calculated when the center of the Sun was 5° above horizon and the angle of incidence was less than 85° to prevent too unrealistic magnifications of direct radiation due to division. The equation 32 assumes that the sky is isotropic which probably is not the case always so it most probably has an effect on the model. Table 3, 4, and 5 show the obtained coefficients for these models.

Table 4: Global irradiation coefficients for a tilted plane in 42 degrees.

n	0	1	2	3	4	5
β_n	-0.584	0.188	69.53	0.768	-7.0×10^{-6}	-57.482
s.e.	0.247	0.002	2.675	0.002	2.78×10^{-6}	2.818
z-score β_n	130.906	60.033	25.526	181.440	-1.895	-20.000
s.e.	0.184	0.717	0.982	0.455	0.750	0.981
p-value	1.8 %	0 %	0 %	0 %	1.2 %	0 %

Table 5: Global irradiation coefficients for a tilted plane in 90 degrees.

n	0	1	2	3	4	5
β_n	1.014	0.247	150.55	0.841	-1.18×10^{-4}	-144.693
s.e.	0.257	0.003	2.763	0.002	4.91×10^{-6}	2.882
z-score β_n	104.831	61.281	55.272	146.201	-18.765	-50.344
s.e.	0.192	0.776	1.014	0.399	0.782	1.003
p-value	0 %	0 %	0 %	0 %	0 %	0 %

3.2 The weather parameters

The input parameters of the model in addition to theoretical irradiance are the sunshine hour and the ambient temperature. To help estimating the available solar irradiance on different times of year, probabilities of sunshine hours in different months were calculated from the data between 1.1.1981–10.7.2011. When considering only the hours of a day when the center of the Sun is above above horizon, the most probable values for sunshine are 0 and 1, other values are quite uniformly distributed between these values. The Figure 1 shows this kind of distribution of sunshine hours in the month of August obtained from the data between 1981–2010. These probabilites might have inaccurateness for example because of the surroundings like trees and buildings around measurement site so although the Sun should be above horizon, it might have been behind the trees. Table 6 presents the probabilities of sunshine hours and the mean value for each month. With the mean value of each month, irradiation of whole year was calculated and it was noticed that the approximately the same result was achieved by using value of 0.437 for sunshine hour for whole year.

When calculating the year energy with the sunshine hour value of 0.437,

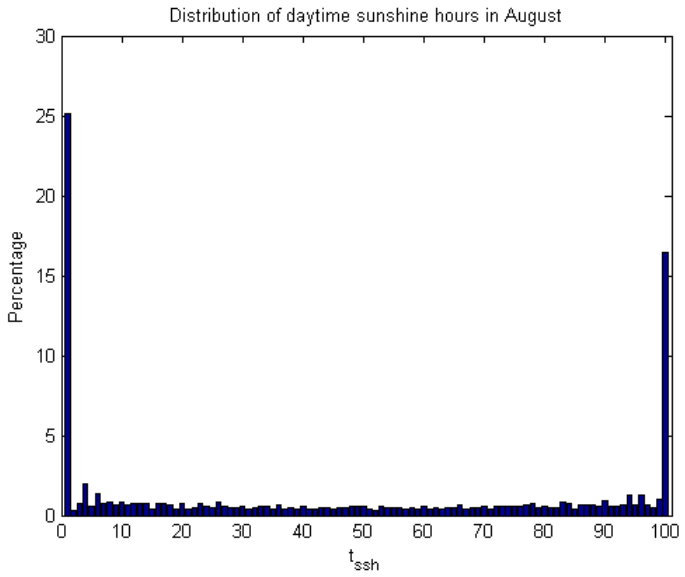

Figure 1: The distribution of daytime sunshine hours of August.

an energy of 985 kWh/m^2 for horizontal surface was obtained. As Figure 2 shows the value is on average 3.6 % higher than the measured year energies. This was achieved by only taking into account the hours when the hourly theoretical values should be above zero. To get more precise values, better resolution of theoretical model and information about the surroundings of the measurement site should probably be known.

To see how the solar energy is distributed through a year, daily irradiation values with different tilt angles was drawn. Figure 3 shows the graphs of three different tilt angles with three different values of sunshine hour. From the graphs can be seen how the shape of the curve varies with different tilt angles. When using the 42° tilted surface, the maximum energy during the midsummer is quite the same as with horizontal but the spring and autumn will give more energy. On the other hand the vertical surface is good during the winter time compared but weak duting the summer compared to others.

With the knowledge of global irradiation, a step to the solar module can be taken. Like the equation 27 shows, the temperature of the cell must be estimated and it depends on ambient temperature. Because the effect

Table 6: The probabilites of constant direct and no sunshine and the monthly weighted mean value of sunshine hour.

Month	$t_{\text{ssh}} = 0$	$t_{\text{ssh}} = 1$	Mean value of t_{ssh}
January	70.3 %	7.9 %	0.179
February	54.9 %	15.7 %	0.297
March	46.7 %	20.4 %	0.366
April	34.3 %	23.9 %	0.452
May	24.7 %	27.2 %	0.518
June	26.3 %	22.4 %	0.490
July	21.7 %	23.0 %	0.526
August	25.2 %	16.4 %	0.456
September	35.8 %	13.4 %	0.375
October	53.1 %	11.2 %	0.273
November	71.5 %	6.9 %	0.165
December	75.2 %	5.6 %	0.142

of the ambient temperature to the power is quite small, it was decided to use one average value for every hour of every day. This makes the desired model to be more simple to use because it has less changeable parameters. The temperature data was measured only on 3 hour intervals till the year 2001 so the missing points were replaced with the previous value. Now the average values for every hour could be calculated from 30 years of data. Most probably the solar module will not change its temperature as fast as the temperature changes hourly so it is decided to use moving average of 3 values. After this, every parameter to estimate hourly energy produced by a solar module is defined and the equation 27 can be used.

3.3 Hourly power generation model

It was decided to construct three different cloudiness cases for each tilt angle. The tilt angles are 0°, 42° and 90°. The power generation for each of these is calculated with three different values of sunshine hours. The sunshine hours t_{ssh} are 0, 1, and 0.437 which produces the realistic average energy of one year. The ambient temperature used was the average temperatures for each hour and from that a moving average of 3 was taken. To make it easy

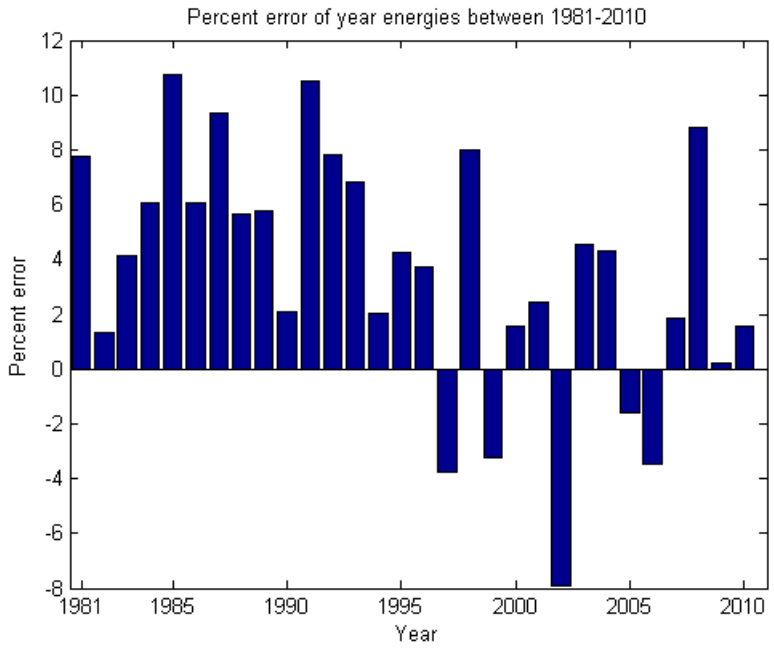

Figure 2: Percent error of year energies between 1981–2010

to estimate the power of a solar module, a table of monthly hourly average values was constructed. An average value for a single hour for every month is calculated so a 12×24 table is obtained from where one can easily get an estimated value and multiply it by the nominal power of the solar module system:

$$P_{\mathrm{m,h}} = \eta_{eff} P_{\max} \frac{p_{\mathrm{index}}}{1000}, \tag{33}$$

where p_{index} is the indexed value from Table 7–15 in Appendix D. The times are all Finland standard time (UTC+2).

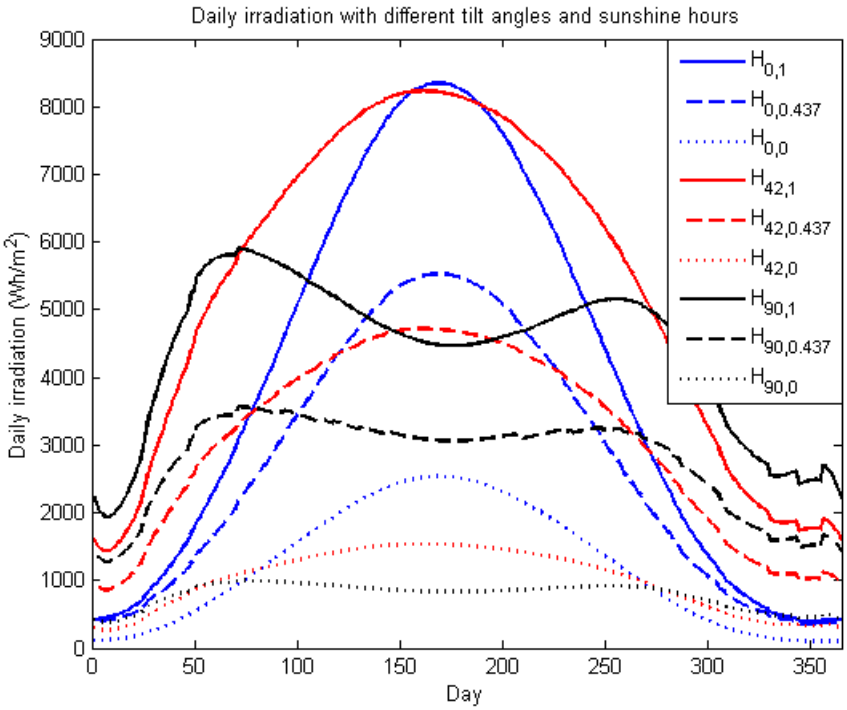

Figure 3: Daily irradiation with different tilt angles and sunshine hours.

4 Model evaluation

4.1 Surface irradiation

In this section the evaluation of the regression model is performed. Like could be seen from the normalized regression coefficients for horizontal surface in Table 3, the p-values of the variable coefficients are under 5 % which makes the variables significant except of the constant term. The normalized coefficients are also quite large values except the value of β_4. To test how the error between the fit function and the measured data handles, all the residual plots of each variables are drawn and they are in Appendix A. Figure 17 shows that the magnitude of residual varies clearly through different seasons being the biggest in summer time.

The error measurements that have not been corrected can also be easily seen from the figures where they differ clearly from the main group of dots. The scatter residual plot of a variable should be a steady horizontal line and not to get wider with any variable value. The residual plots show that most of them do get little wider in the ends but not very greatly. The residual plot of theoretical irradiance G_{glob} in Figure 19 gets wider on larger values. Also the residual plot of H_{fit} in Figure 18 has an interesting widening in the beginning which then disappears and the rest is very steady line. This is most probably because our model can not handle the different diffuse radiation values when the value of sunshine hour is zero. It suggests that there would most probably be at least one explanatory variable that would make the model better.

The residual plots of the 42° and 90° tilted surfaces in Appendix B and C show similar results compared to those for the horizontal surface although the residuals are larger and the shapes of the curves are not as smooth. Especially the case of 90° tilted surface has significantly weaker residual plots than the others.

The autocorrelations of the hourly residuals with lags 1–30 is shown in Figures 4, 6, and 8. It can be seen that the previous hours have an effect on the present estimation which seems quite logical as the amount of sunshine is probably quite at the same level as in the previous hour. When calculating the autocorrelation of the daily residual sums, it is quite interesting to notice the little bigger value at the lag of 30 and 31 (Fig. 5). It looks like something

in the model changes monthly. One possibility might be the values of Linke turbidity values that were monthly but interpolated to get daily values.

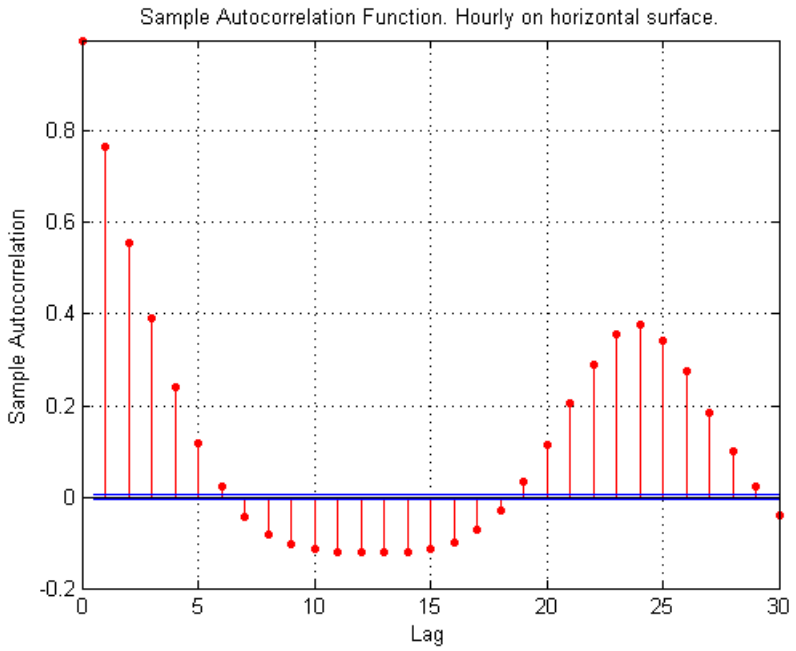

Figure 4: Autocorrelation of the hourly residuals with lags 1–30.

Figure 10 shows how the model fits the measured data quite typically in the case of horizontal irradiation. It can be seen that the first day is quite clear, the second is mostly cloudy and the last is fully cloudy. The model usually follows the changing irradiation quite well like seen in the first and the second day. The weakest fitting is always on very cloudy days when the radiation is very low and the model does not follow the shape of the irradiation and therefore gives too large values like in the third day. As the sunshine hour value is zero, the cloudiness may be thin or thick especially if it is raining, the irradiation is very low. Figures 11 and 12 show the fittings of the tilted models on the same days as for the horizontal surface. These models have more variation since the actual measurement data is for the horizontal surface and had to be manipulated with equations 31 and 32 to get the estimation of tilted surface irradiation.

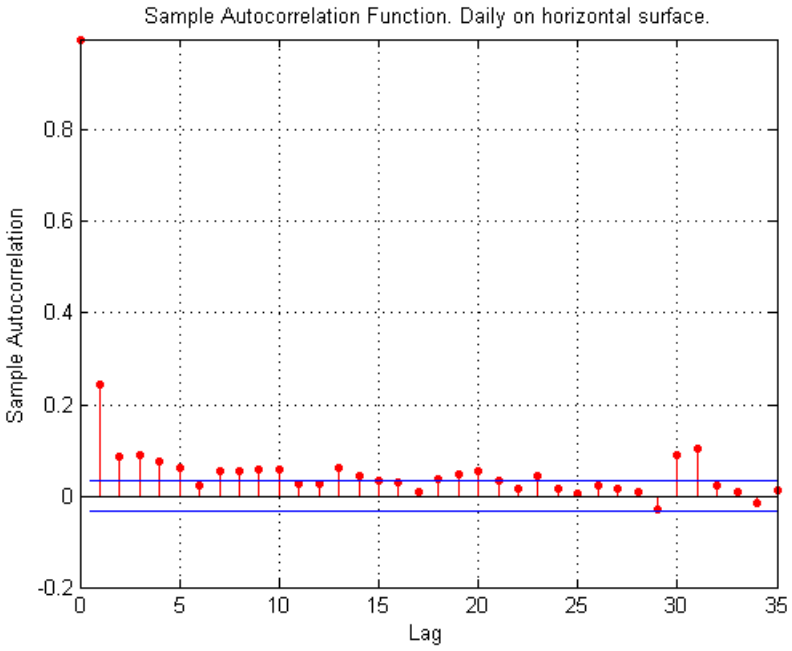

Figure 5: Autocorrelation of the daily residuals with lags 1–35.

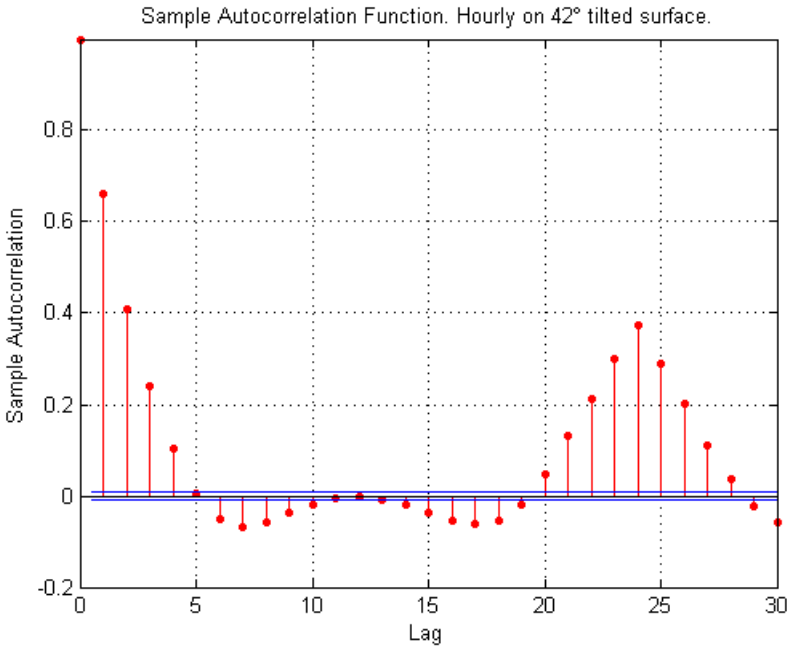

Figure 6: Autocorrelation of the hourly residuals with lags 1–30.

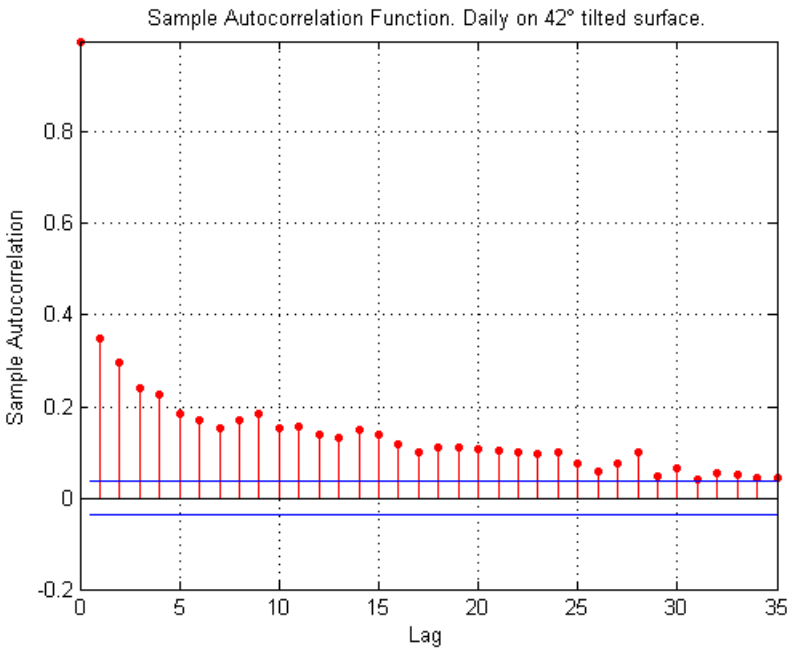

Figure 7: Autocorrelation of the daily residuals with lags 1–35.

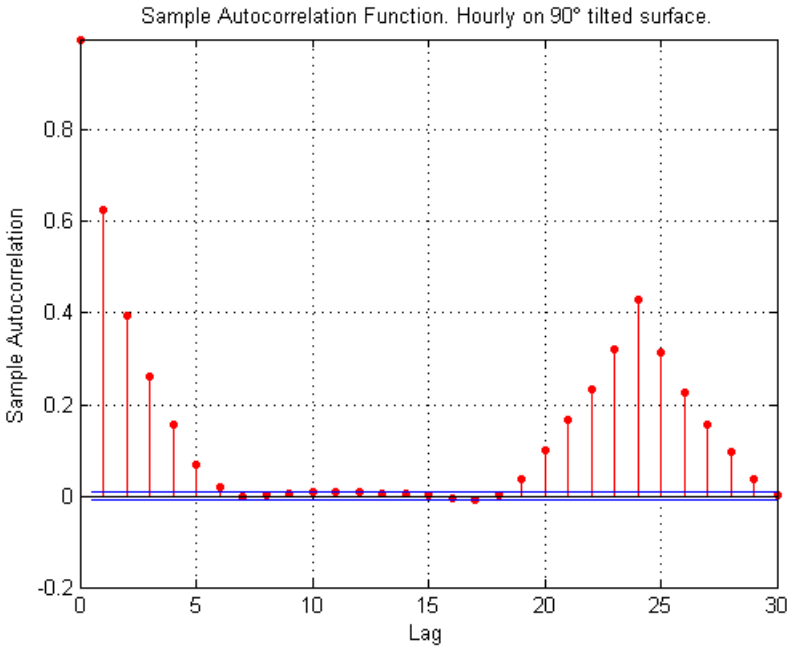

Figure 8: Autocorrelation of the hourly residuals with lags 1–30.

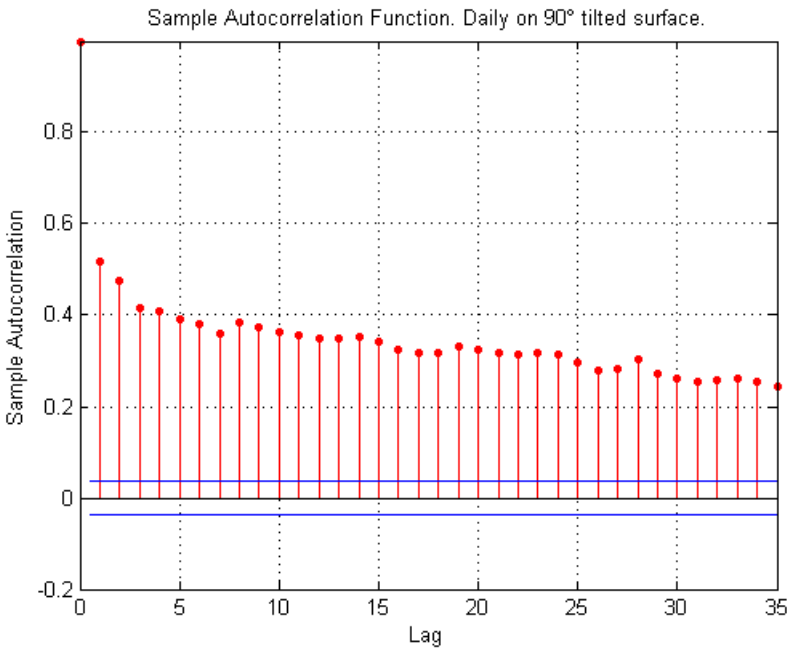

Figure 9: Autocorrelation of the daily residuals with lags 1–35.

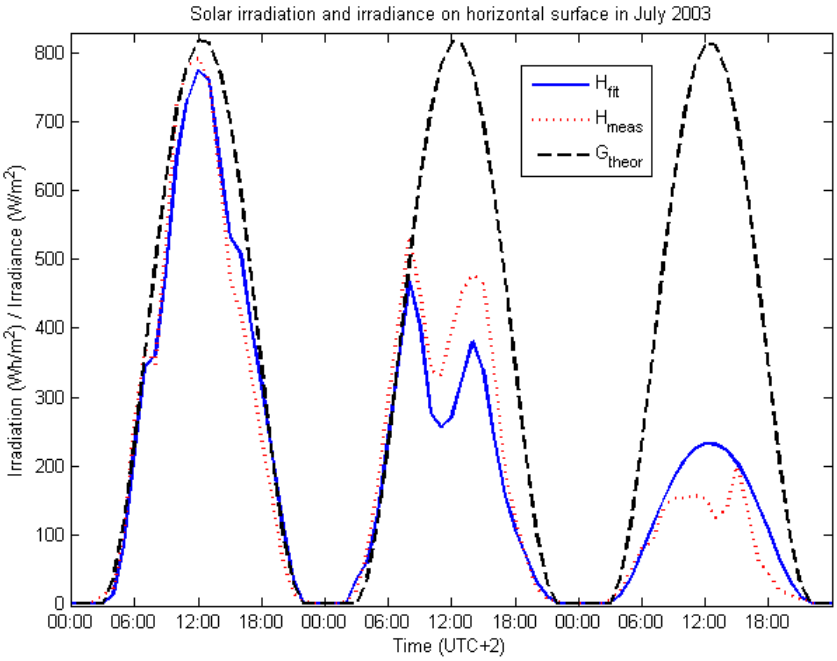

Figure 10: Graphs of theoretical irradiance values, measured irradiation data and the modelled irradiation on horizontal surface between 3 days.

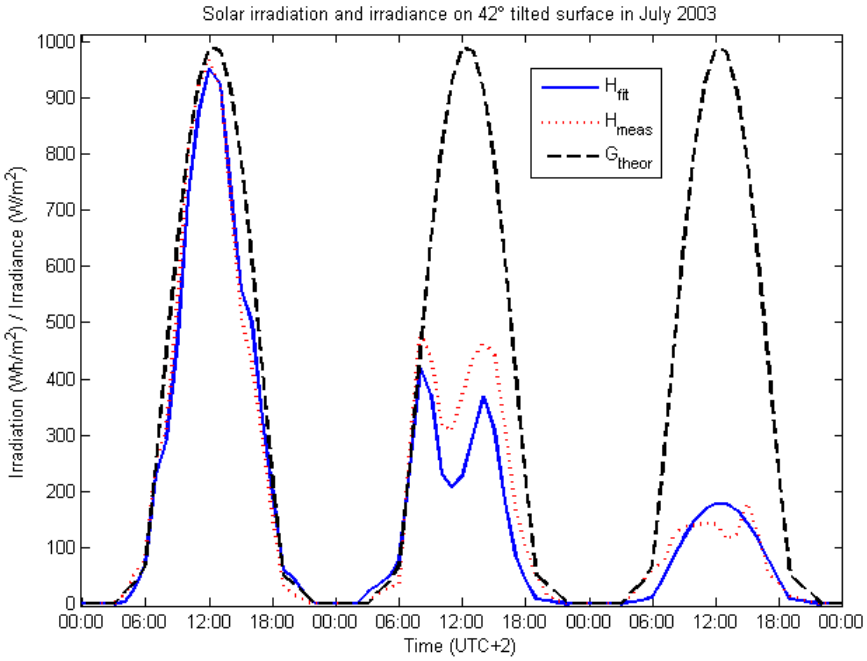

Figure 11: Graphs of theoretical irradiance values, measured irradiation data and the modelled irradiation on 42° tilted surface between 3 days.

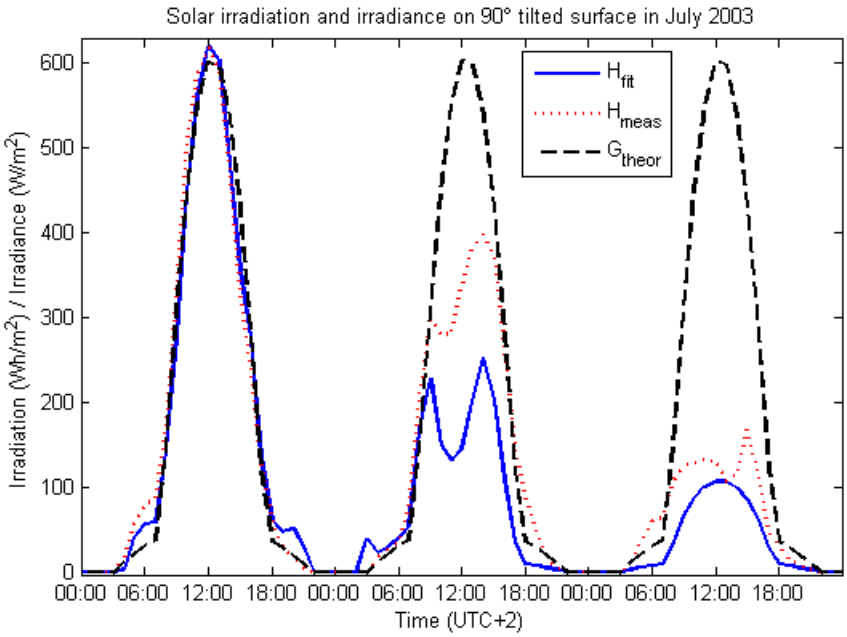

Figure 12: Graphs of theoretical irradiance values, measured irradiation data and the modelled irradiation on 90° tilted surface between 3 days.

4.2 Power output

The model for power generation is quite simple but it is not used as most precise method as possible. The solar module will not provide energy with good efficiency in cases when irradiance is less than 100 W/m^2. This is usually the case in the morning and evening. An another unmodeled factor that effects the same parts of the day is the transmittance of the solar radiation when the angle of incidence is large. The module surface will reflect most of the radiation in these type of conditions. It was also assumed that the module would always work in maximum power point because of an inverter, which might not be the case in less optimal solar irradiance conditions.

The presented model was fixed to the case that the module would be installed so that free airflow could go under it. An usual case for installation of multiple modules by consumers is installating them to the roof of their house. This would increase the module temperature because it prevents the airflow from cooling the backside of the module and thus decreasing te efficiency. The wind was also neglected from the module temperature model.

Figures 13, 14 and 15 show how much energy does the module produce per month on average compared to the theoretical maximum. Especially it is interesting to notice how the case of 42° tilt angle the available energy in spring and autumn is very large compared to the amount that module could get realistically. This effect then can be seen when calculating the yearly energies which is in Figure 16. The theoretical maximum energy changes quite a lot with different tilt angles but the average does not increase that much.

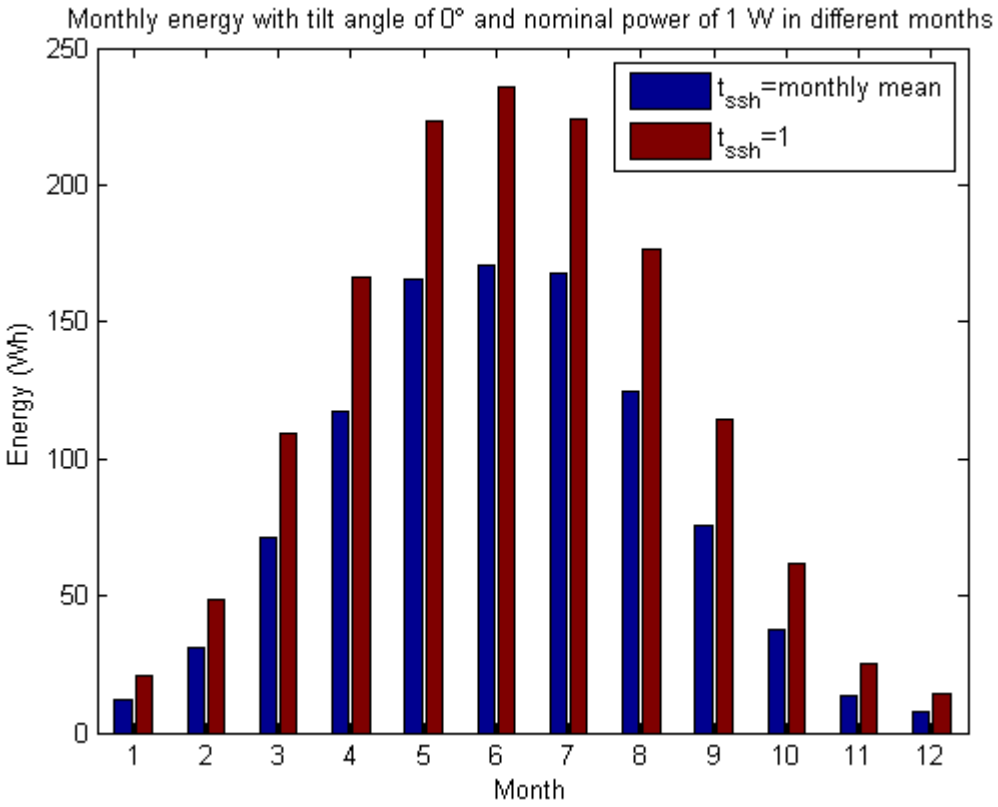

Figure 13: Montly energy with tilt angle of 0° and nominal power of 1 W in different months.

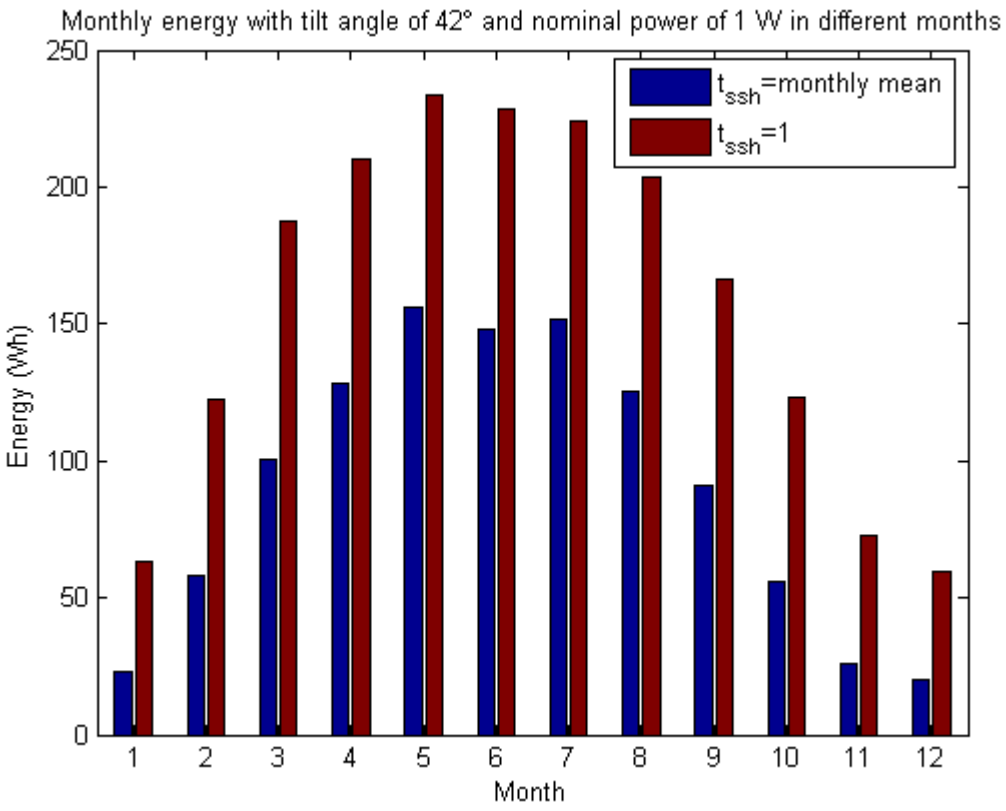

Figure 14: Montly energy with tilt angle of 42° and nominal power of 1 W in different months.

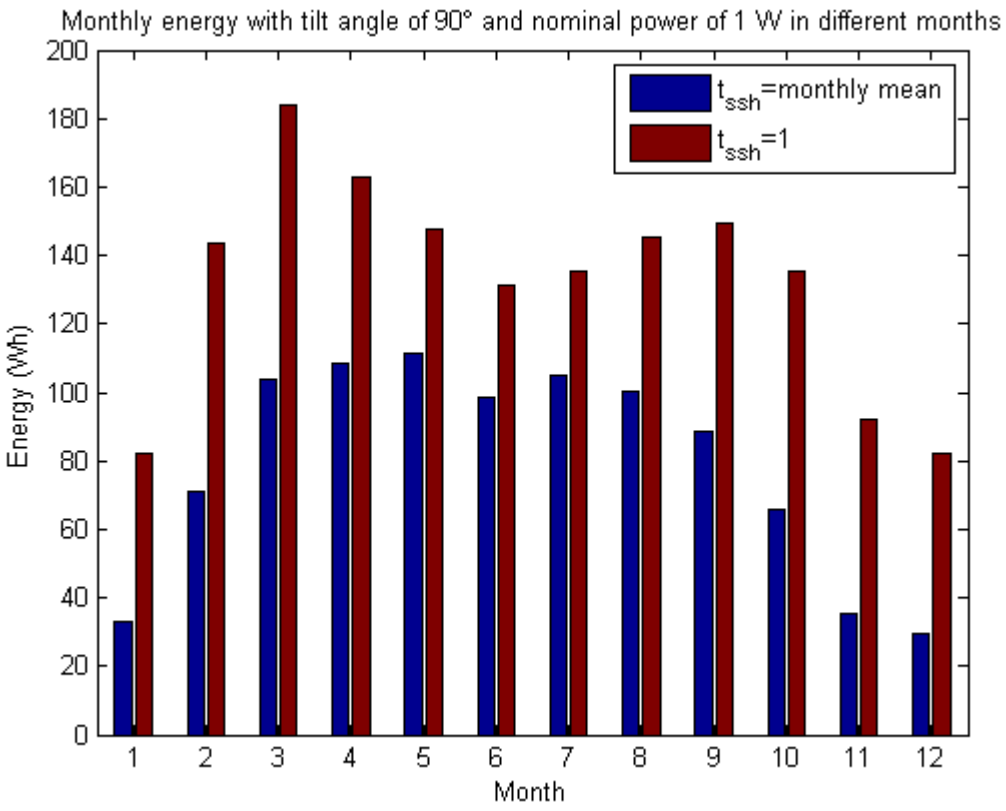

Figure 15: Montly energy with tilt angle of 90° and nominal power of 1 W in different months.

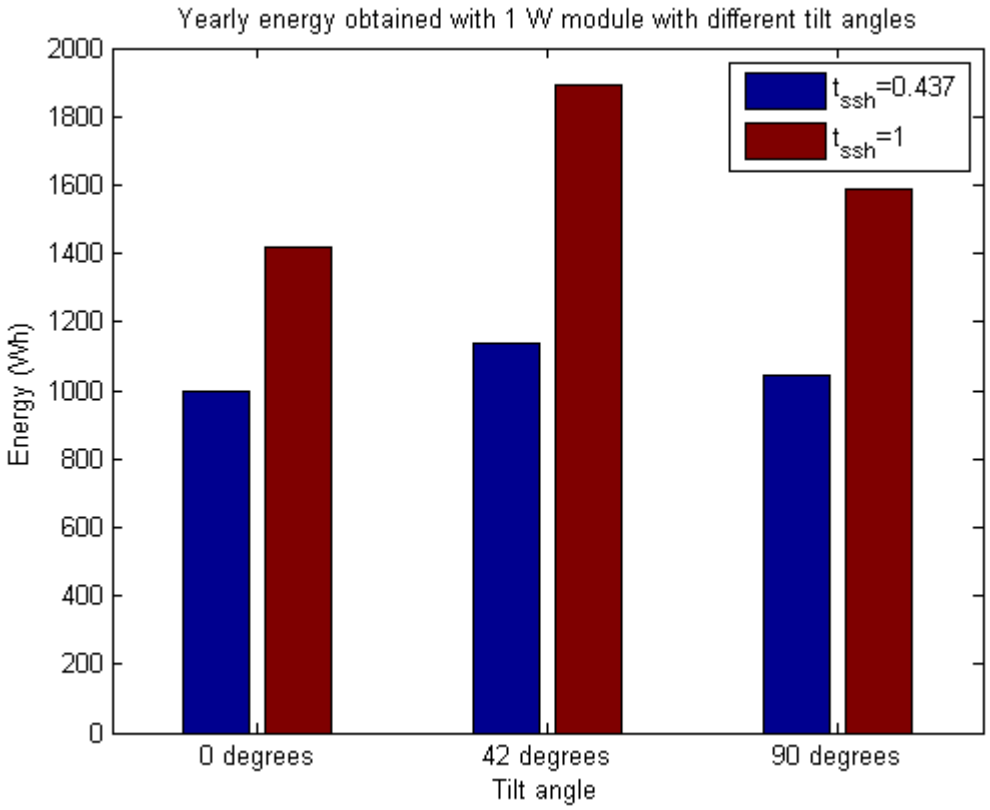

Figure 16: Yearly energy obtained with 1 W module with different tilt angles.

5 Conclusions

In this work, a solar module model that would estimate the available energy in different sunshine conditions was constructed. With the final model also monthly average values of different times of a day were calculated and presented in table to easily obtain an estimation of available solar energy.

The irradiation model presented in this work is very significant part of the solar module model and it is important that it would be as precise as possible. In this model some simplifications were made e.g. a theoretical solar irradiance was used instead of theoretical irradiation which is also presented by Rigollier et al. [4] but it is little more complex. The Linke turbidity factor for an air mass 2 affects greatly to the theoretical values of irradiance in this model and those values could be estimated with more care.

The power output model has some weaknesses because of its simplicity. Obviously the decision to use only one hourly average ambient temperature causes an inaccuracy in the output value. Most probably the ambient temperature is higher during summer time when the sky is clear and the Sun is shining and lower when it is not. Although it is important that the equation of the cell temperature takes into account the higher temperature of the cell when the Sun is shining. The power produced by the model shortly after sunrise and before sunset should also be considered with care because it is very likely that in real module location the horizon is not clear and it will not get direct sunshine during that time. Also the module has very poor transmittance with high angles of incidence as seen in Section 2.3.

The probabilities of the sunshine must be used with consideration. The probabilities in Table 6 are just the distribution of the sunshine hours. When estimating the sunshine of one day, one should be aware that the probability of an hour is most probably not independent of the previous hour. An another significant aspect for solar power in Finland is winter. Although it should be possible to get some power from the solar modules, it is quite common that even in southern Finland snow covers the ground and the modules and no energy is produced unless the modules are cleared of snow.

The most interesting part of this work is obviously the information of available solar power. In this work no verification of the power output of the module is presented. It would be important to get good measurement data

of a solar module power generation to compare the results with our model. Combined with weather and irradiation data an interesting regression analysis for the produced energy could be achieved.

References

[1] Luque, Antonio & Hegedus, Steven. *Handbook of Photovoltaic Science and Engineering*. John Wiley & Sons, 2003. Available from: http://www.knovel.com/web/portal/browse/display?_EXT_KNOVEL_DISPLAY_bookid=1081\&VerticalID=0

[2] Duffie, John A. & Beckman, William A. *Solar engineering of thermal processes.* Hoboken, NJ: Wiley, 2006. ISBN 0-471-69867-9 (inb.), ISBN 978-0-471-69867-8

[3] Mattei M. & Notton G. & Cristofari C. & Muselli M. & Poggi P. *Calculation of the polycrystalline PV module temperature using a simple method of energy balance*, Renewable Energy, Volume 31, Issue 4, April 2006, Pages 553-567, ISSN 0960-1481, DOI: 10.1016/j.renene.2005.03.010. Available from: http://www.sciencedirect.com/science/article/pii/S096014810500073X

[4] Christelle Rigollier, Olivier Bauer, Lucien Wald, *On the clear sky model of the ESRA – European Solar Radiation Atlas – with respect to the heliosat method*, Solar Energy, Volume 68, Issue 1, January 2000, Pages 33-48, ISSN 0038-092X, DOI: 10.1016/S0038-092X(99)00055-9. http://www.sciencedirect.com/science/article/pii/S0038092X99000559

[5] SoDa - Solar radiation data. [homepage on the Internet].[updated 2011 July 28; cited 2011 August 1]. Available from: http://www.soda-is.com/eng/services/climat_free_eng.php\#lin

[6] Finnish Meteorological Institution. Helsinki-Vantaa airport weather data 01.01.1981–10.07.2011.

A Residual plots of the horizontal surface global irradiation model

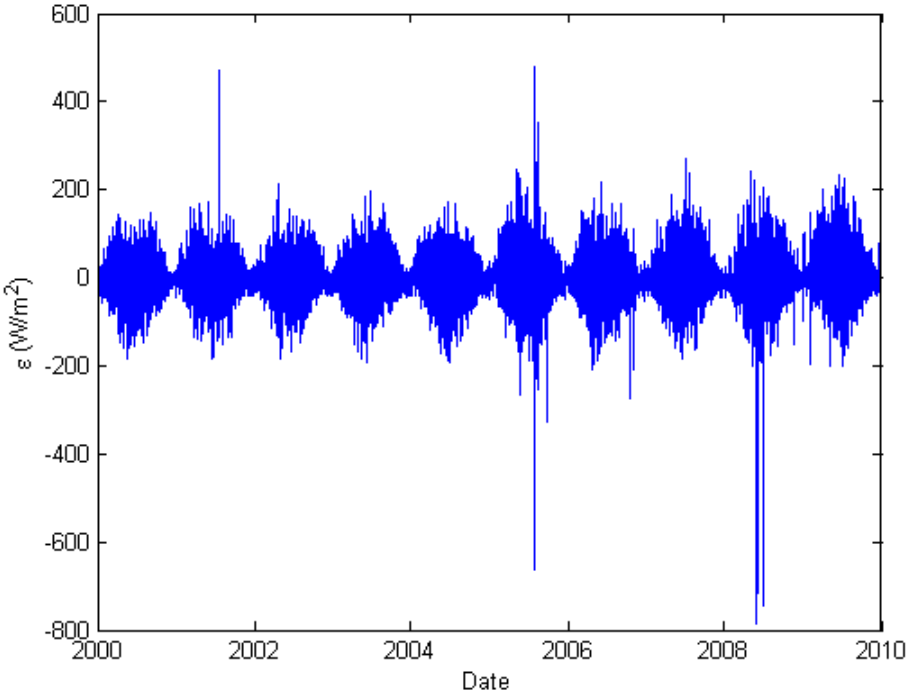

Figure 17: Residuals against time on horizontal surface.

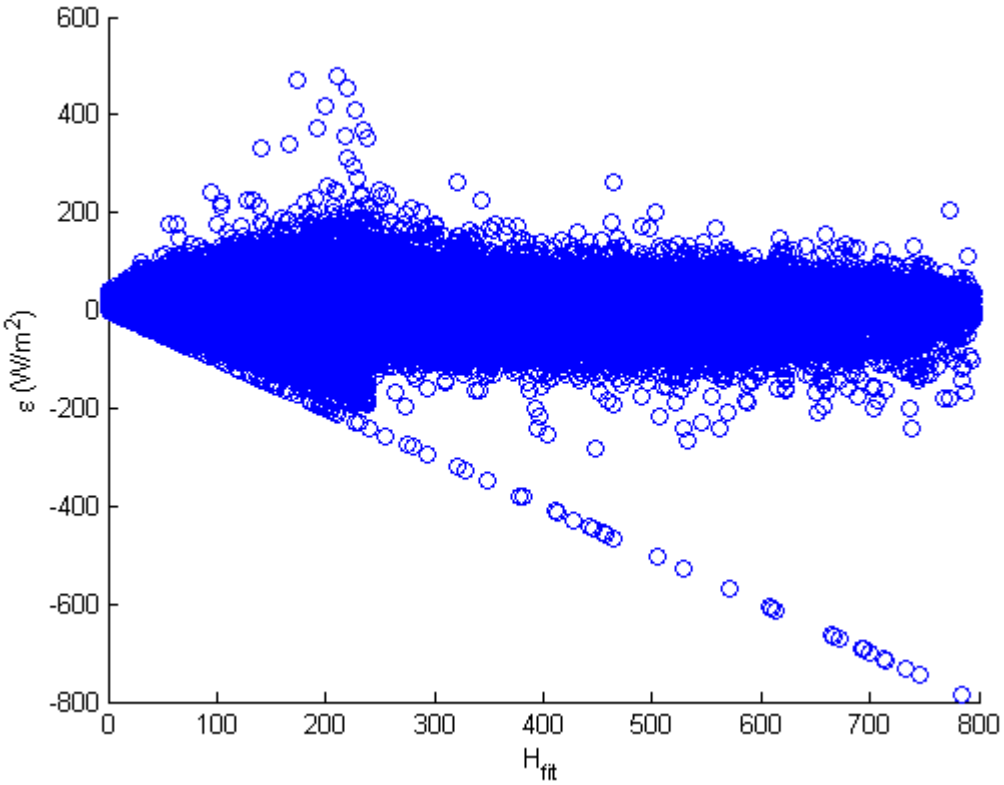

Figure 18: Residual plot of H_{fit} on horizontal surface.

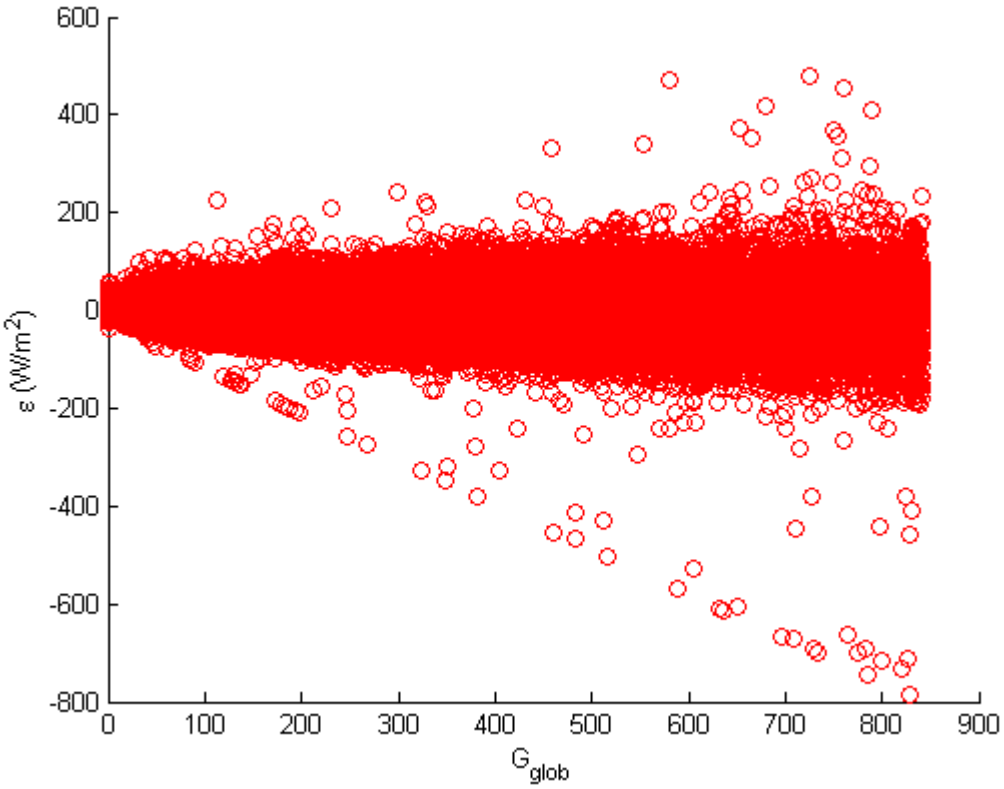

Figure 19: Residual plot of G_{glob} on horizontal surface.

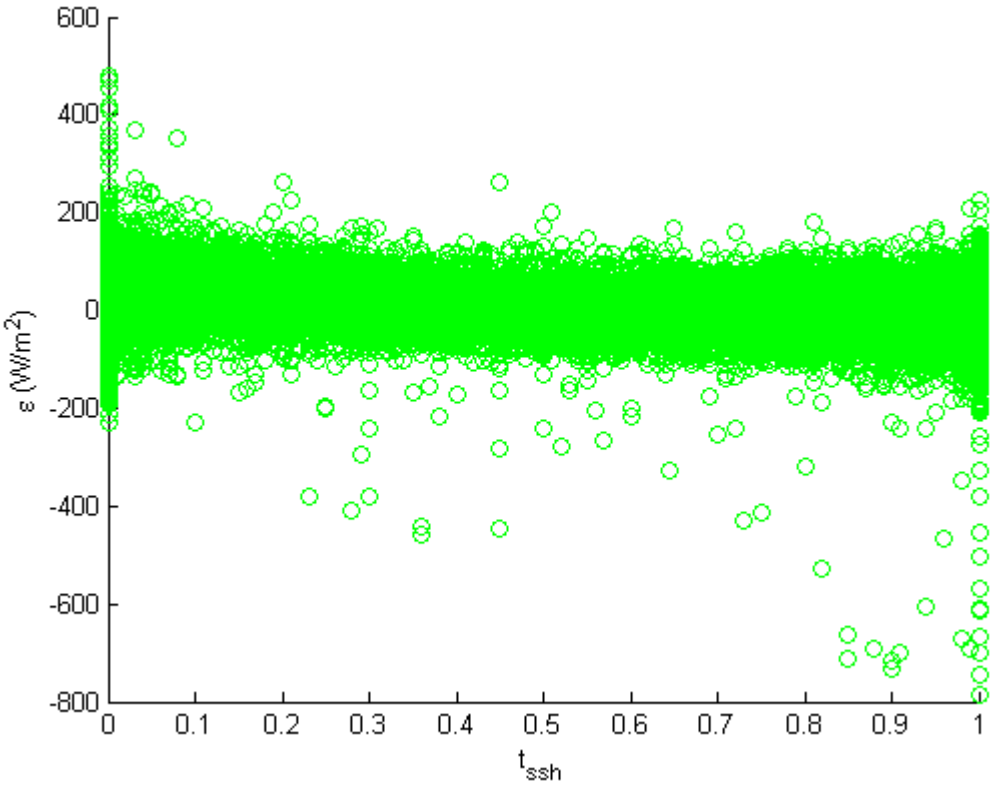

Figure 20: Residual plot of t_{ssh} on horizontal surface.

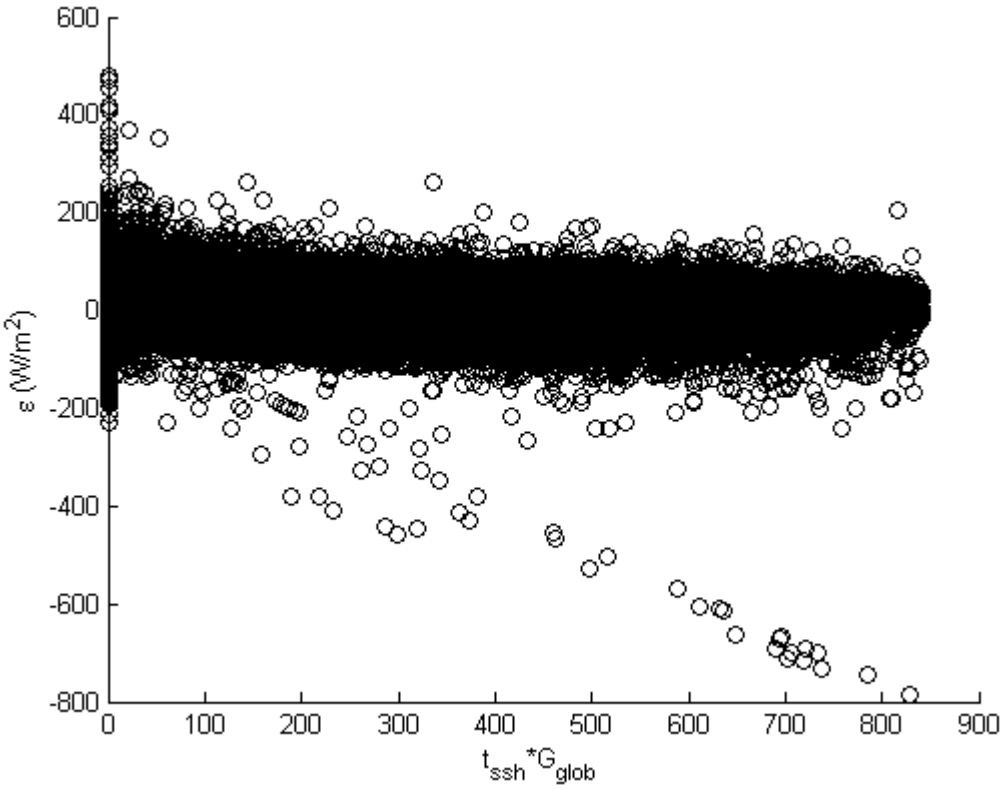

Figure 21: Residual plot of $G_{\mathrm{glob}} t_{\mathrm{ssh}}$ on horizontal surface.

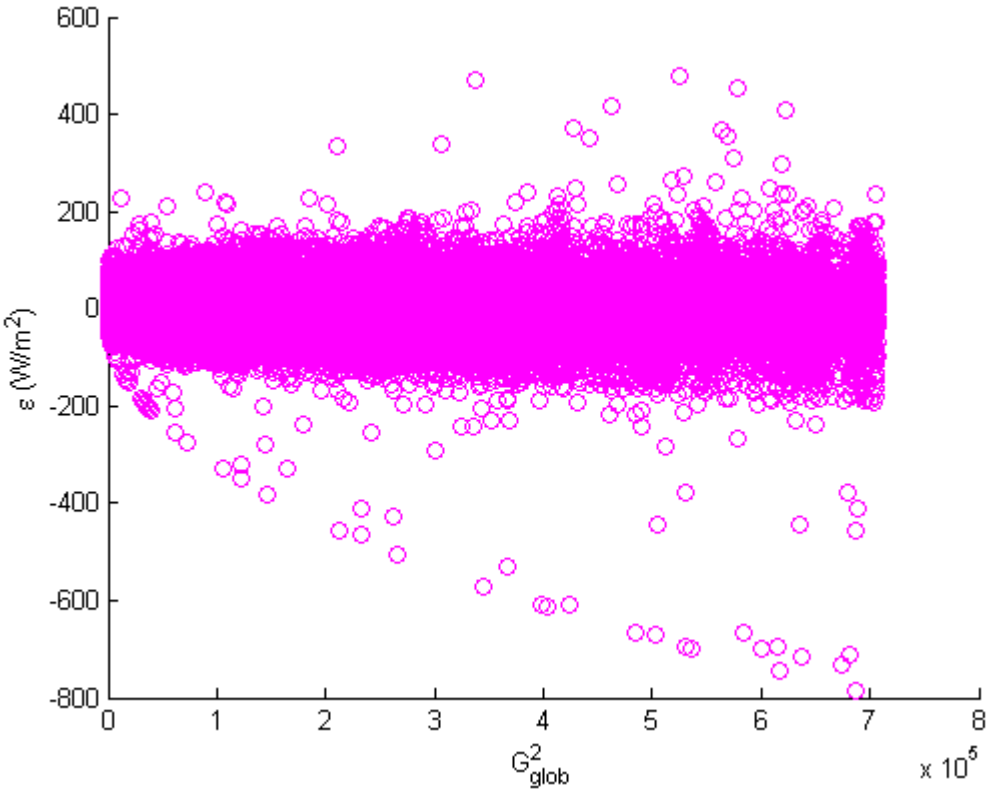

Figure 22: Residual plot of G^2_{glob} on horizontal surface.

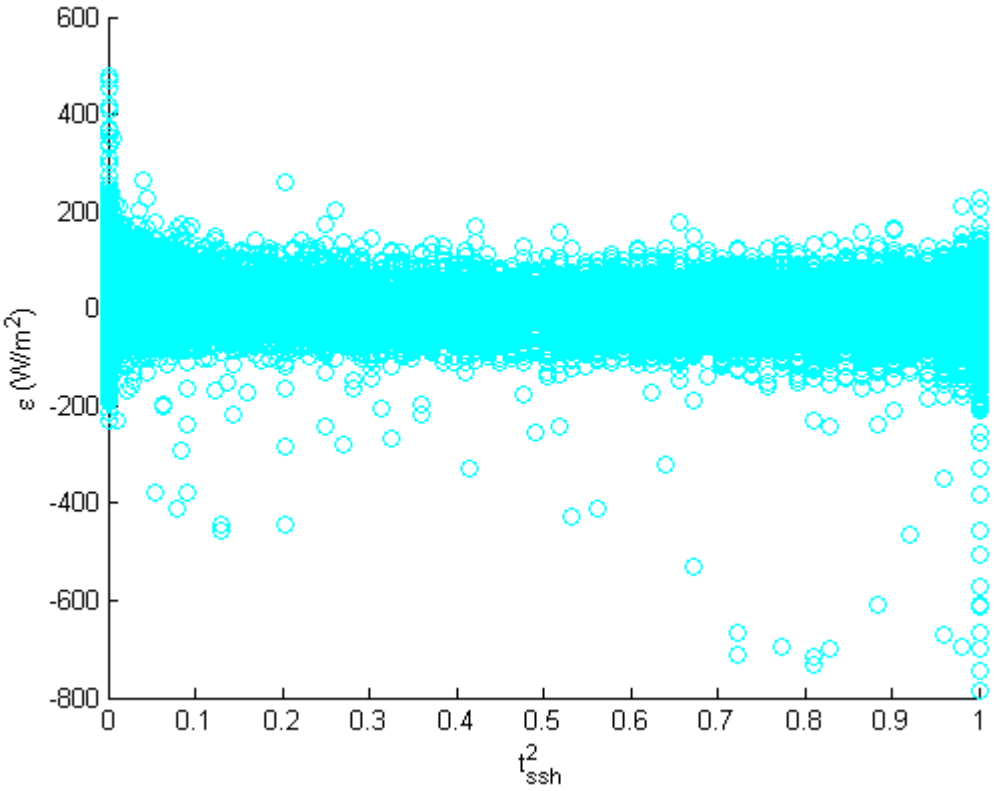

Figure 23: Residual plot of t^2_{ssh} on horizontal surface.

B Residual plots of the 42° tilted surface global irradiation model

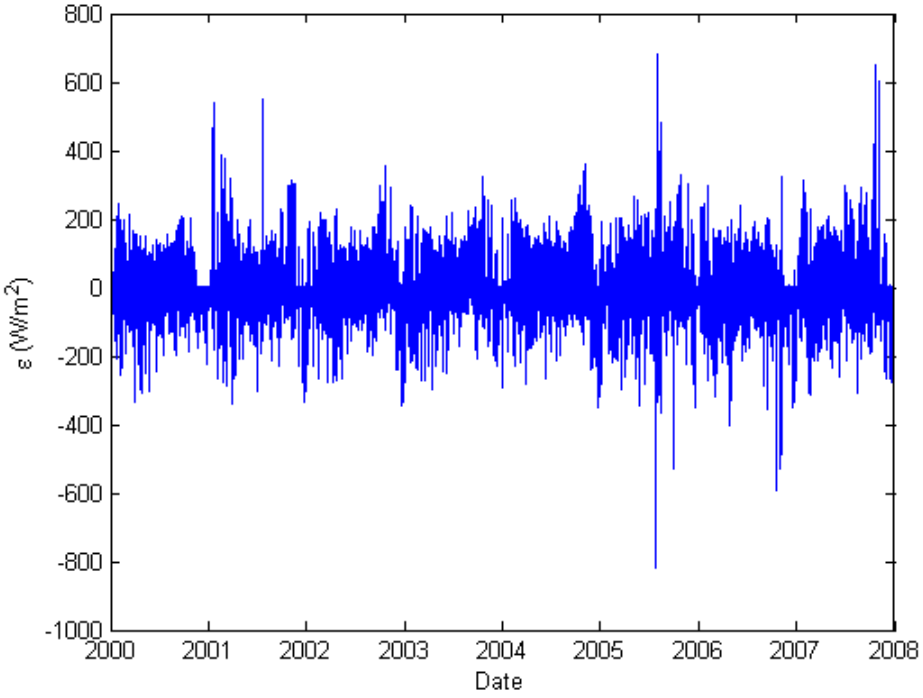

Figure 24: Residuals against time on 42° tilted surface.

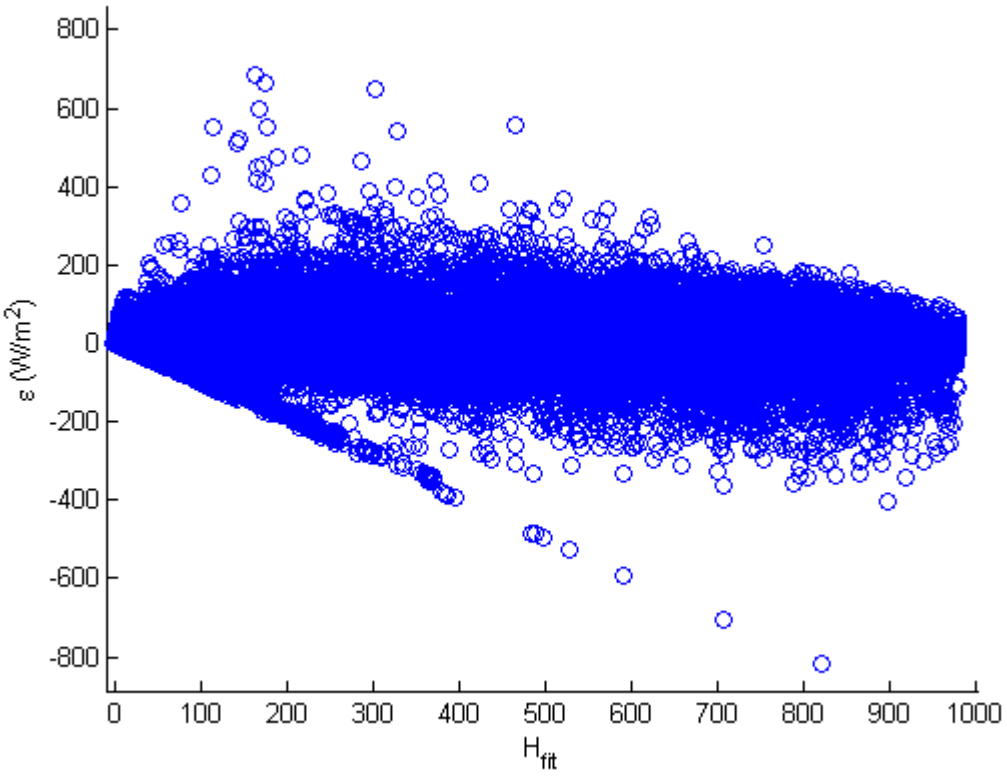

Figure 25: Residual plot of H_{fit} on 42° tilted surface.

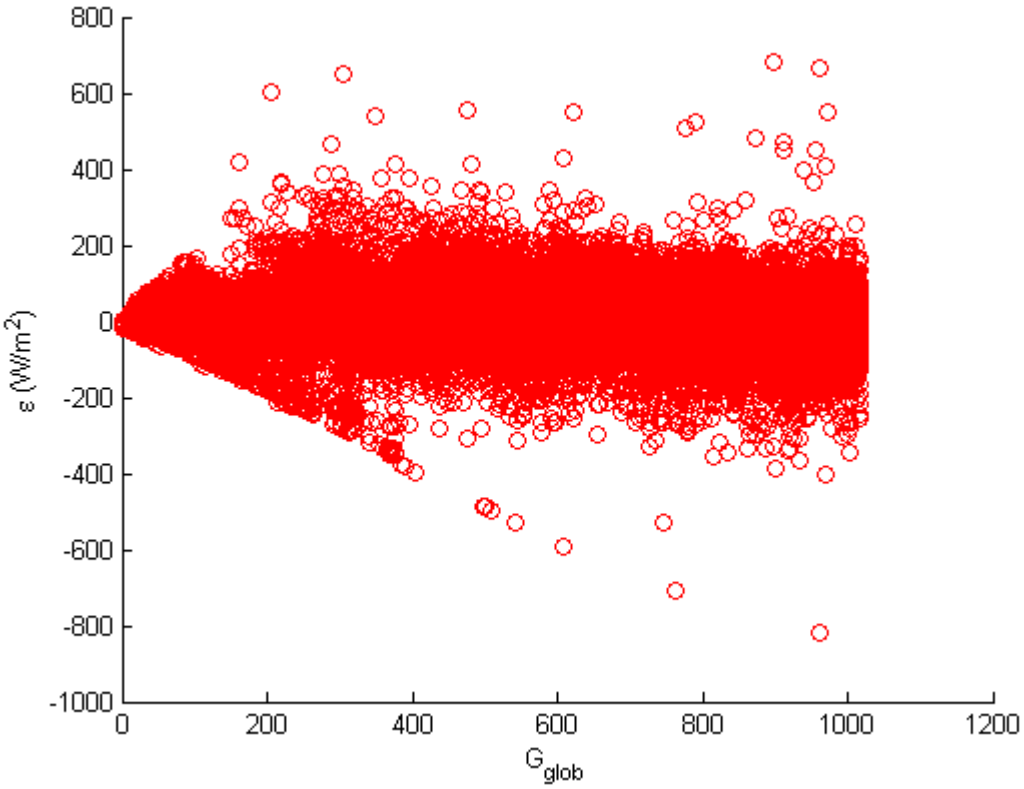

Figure 26: Residual plot of G_{glob} on 42° tilted surface.

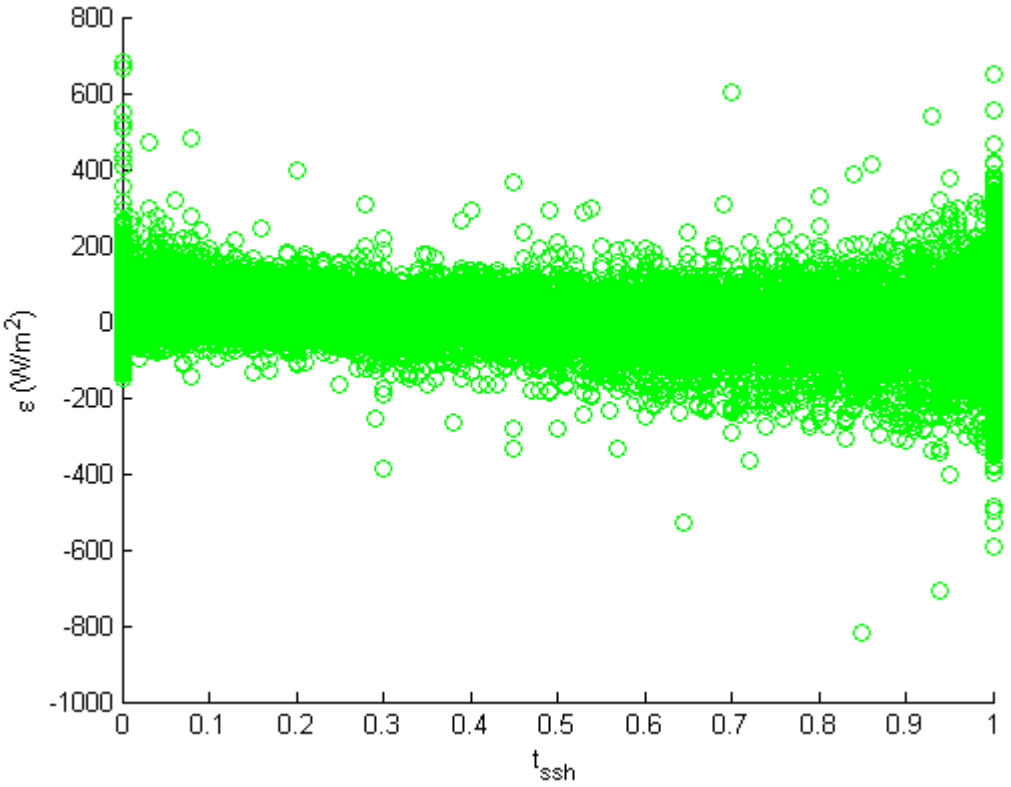

Figure 27: Residual plot of t_{ssh} on 42° tilted surface.

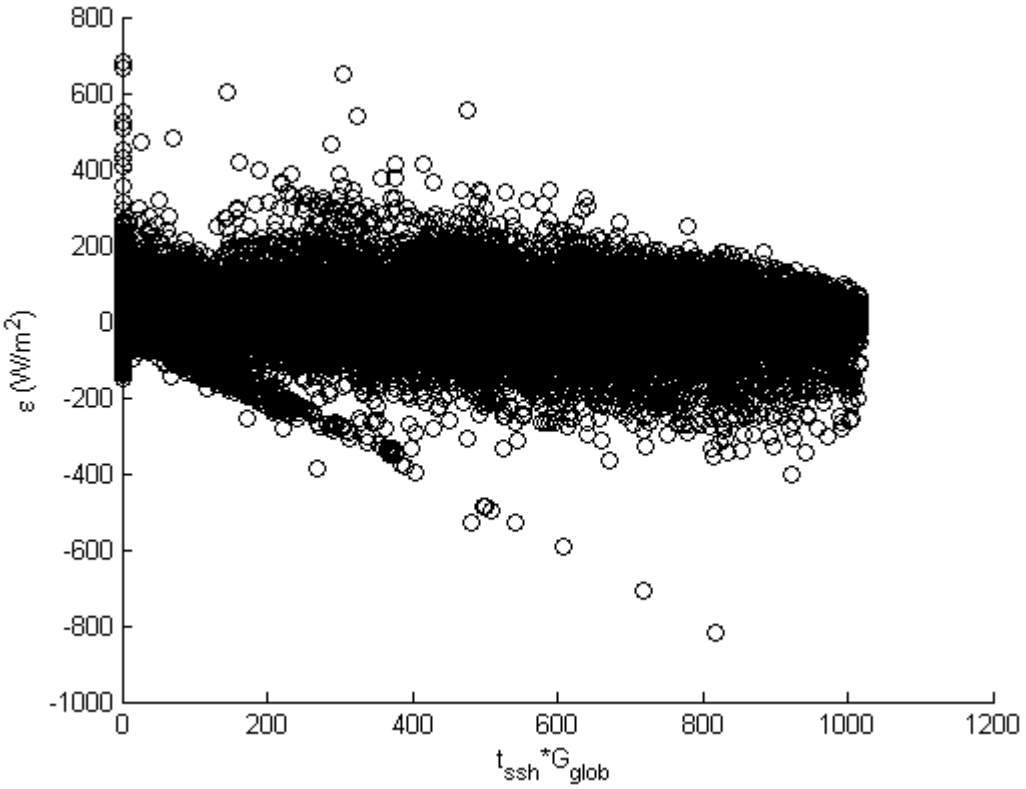

Figure 28: Residual plot of $G_{\text{glob}}t_{\text{ssh}}$ on 42° tilted surface.

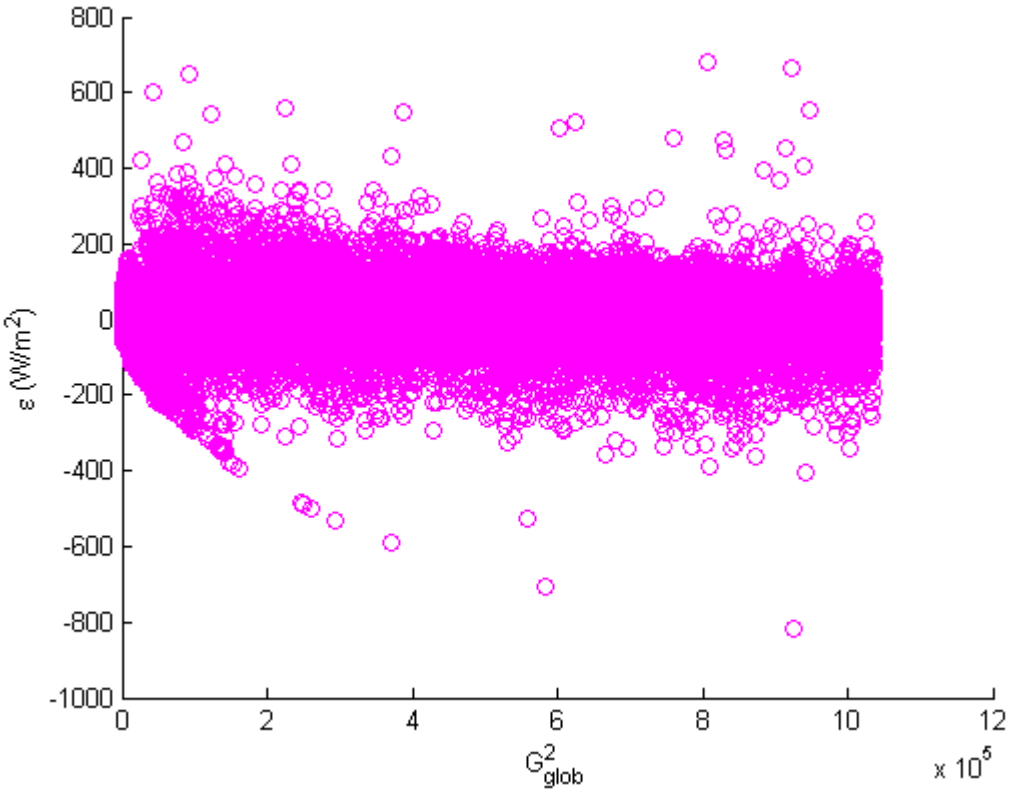

Figure 29: Residual plot of G^2_{glob} on 42° tilted surface.

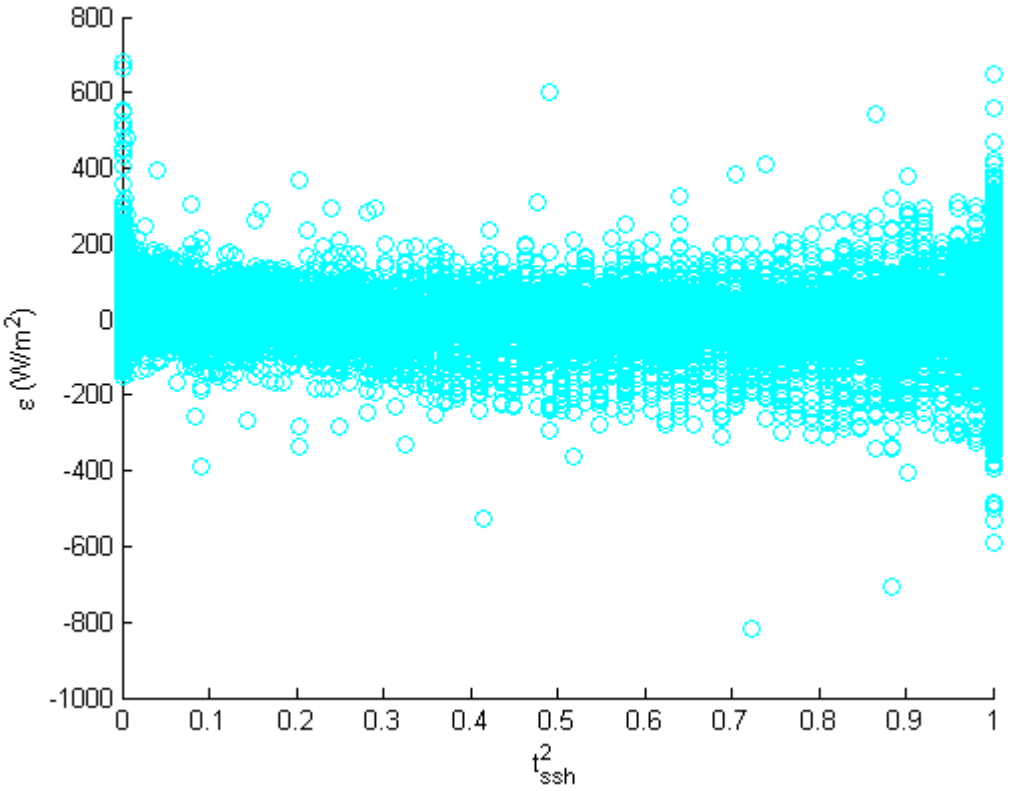

Figure 30: Residual plot of t^2_{ssh} on 42° tilted surface.

C Residual plots of the 90° tilted surface global irradiation model

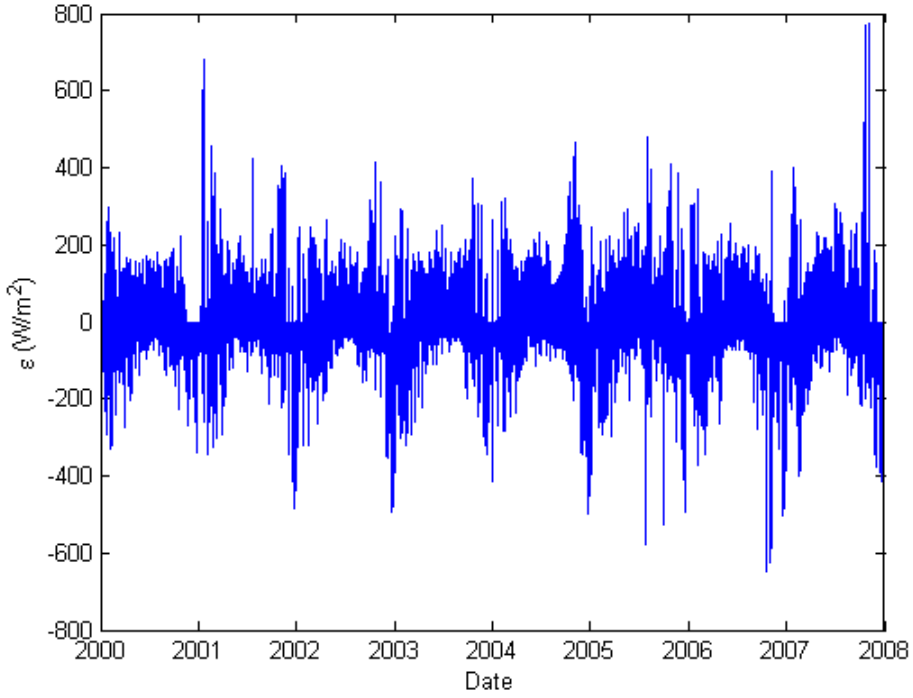

Figure 31: Residuals against time on 90° tilted surface.

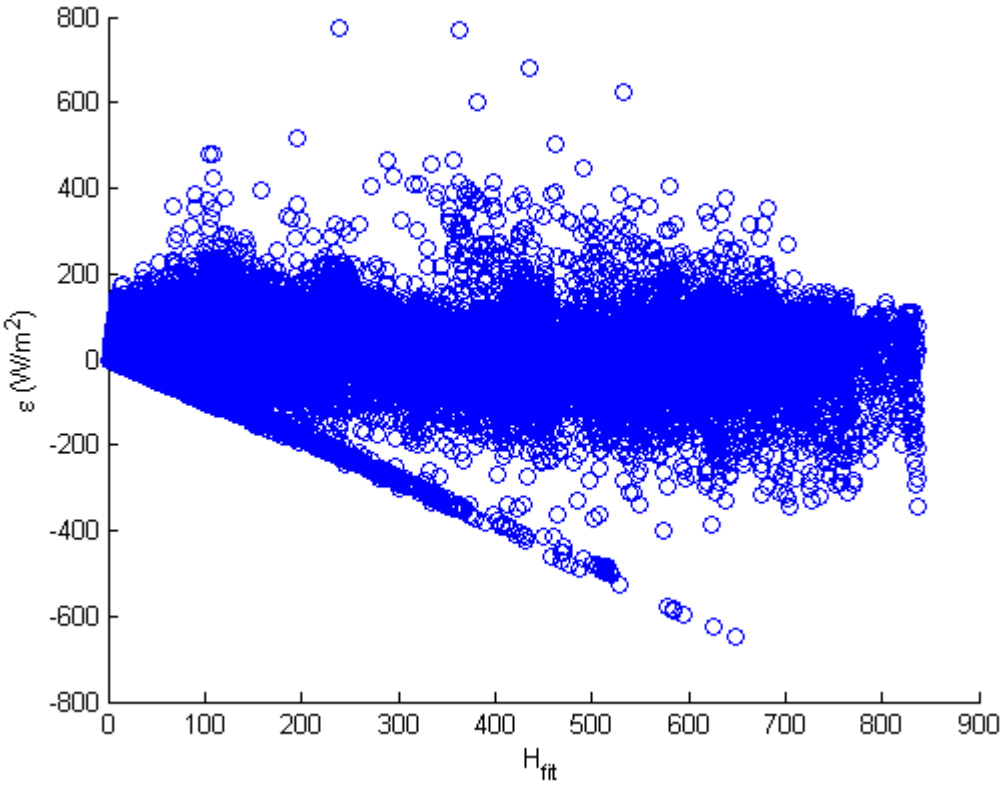

Figure 32: Residual plot of H_{fit} on 90° tilted surface.

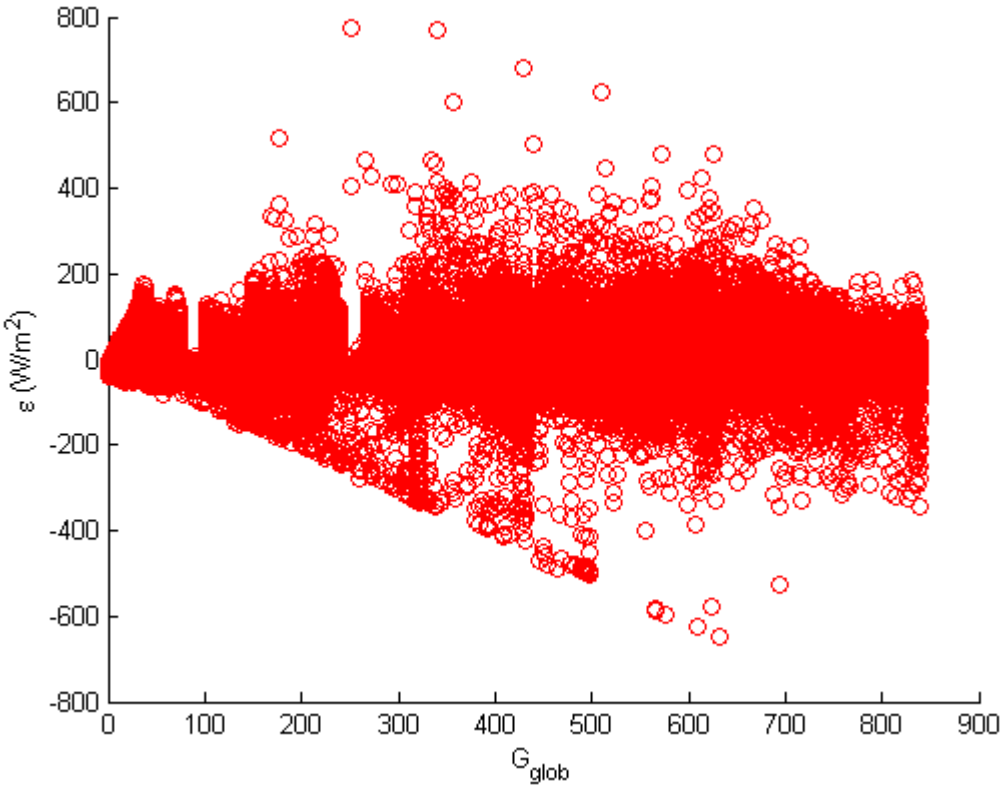

Figure 33: Residual plot of G_{glob} on 90° tilted surface.

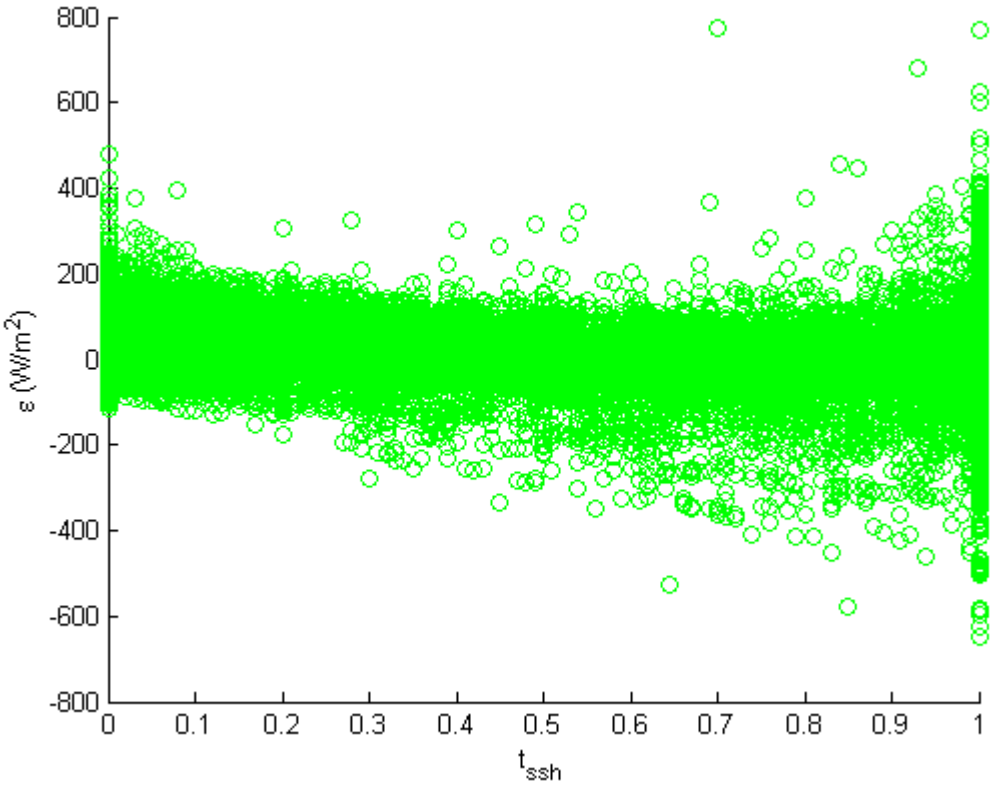

Figure 34: Residual plot of t_{ssh} on 90° tilted surface.

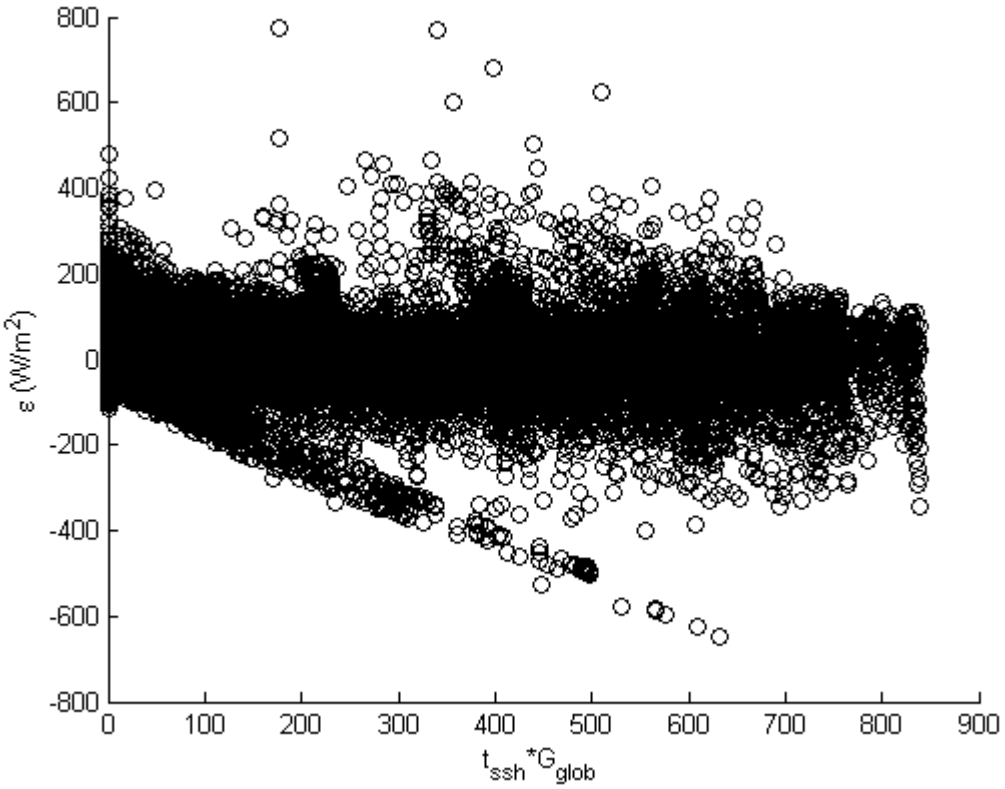

Figure 35: Residual plot of $G_{\mathrm{glob}}t_{\mathrm{ssh}}$ on 90° tilted surface.

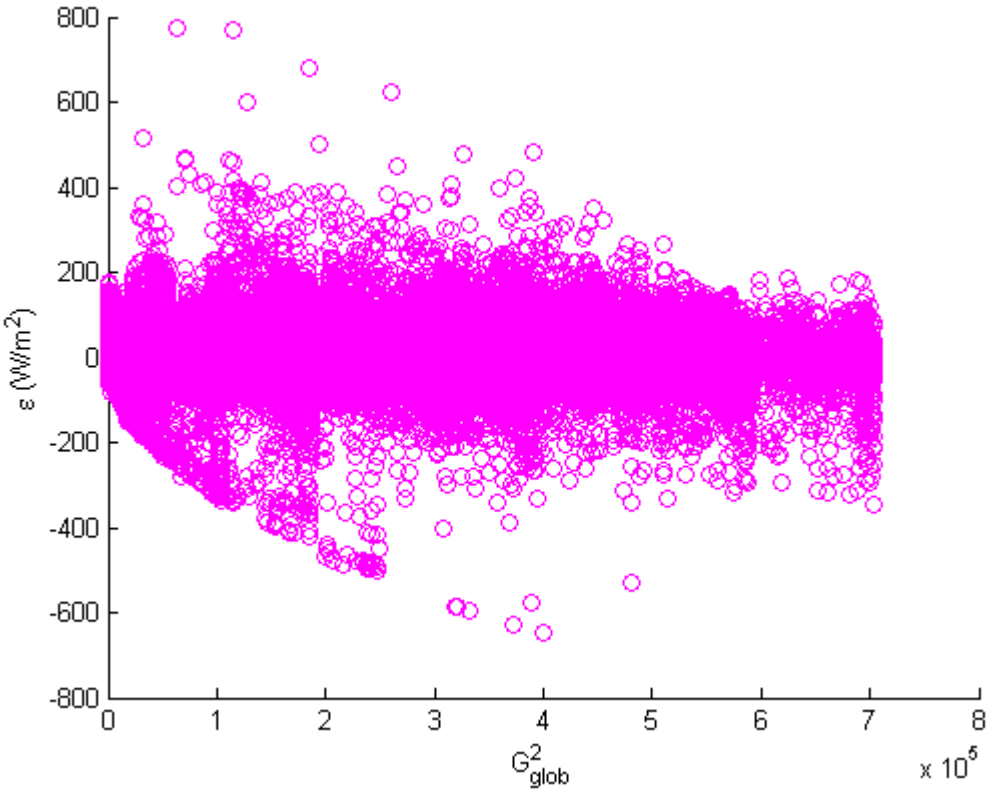

Figure 36: Residual plot of G^2_{glob} on 90° tilted surface.

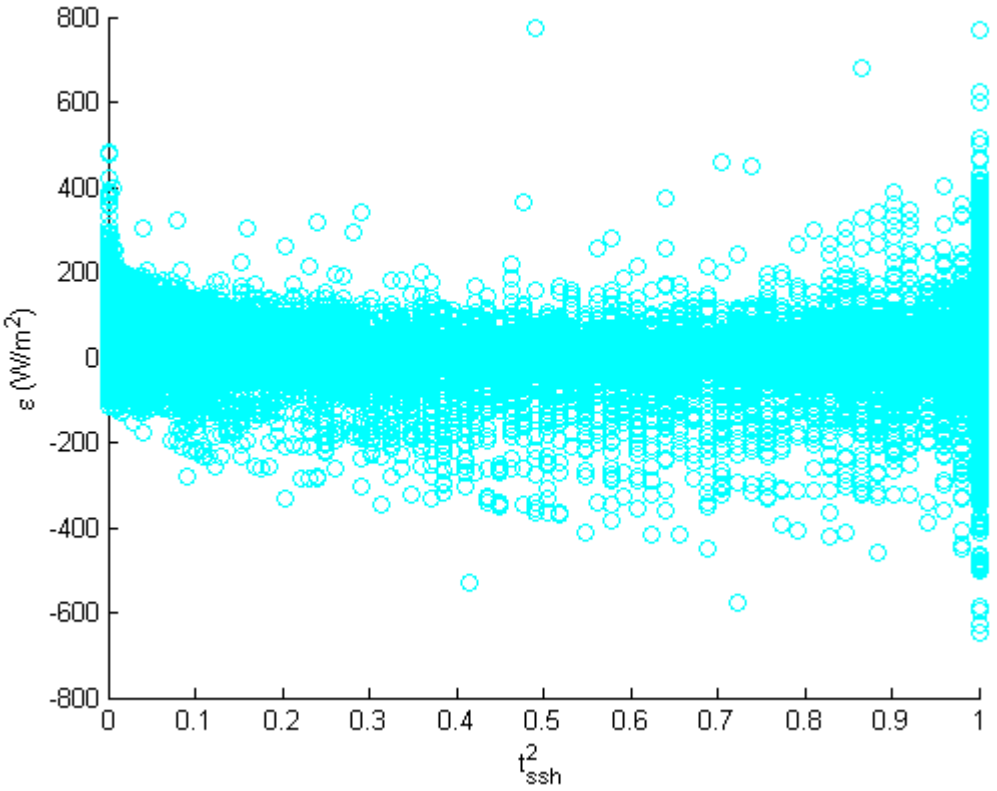

Figure 37: Residual plot of t^2_{ssh} on 90° tilted surface.

D Power index

Table 7: Horizontal $t_{ssh} = 0$

M/h	0	1	2	3	4	5	6	7	8	9	10	11	12	13	14	15	16	17	18	19	20	21	22	23
J	0	0	0	0	0	0	0	0	0	0.94	16.0	32.4	42.4	42.2	32.0	15.6	1.50	0	0	0	0	0	0	0
F	0	0	0	0	0	0	0	0	2.86	25.8	56.9	81.8	95.3	96.0	83.8	60.2	29.6	4.45	0	0	0	0	0	0
M	0	0	0	0	0	0	0.15	11.7	45.7	86.5	121	145	157	156	143	119	84.2	43.7	9.82	0	0	0	0	0
A	0	0	0	0	0	3.46	26.0	66.2	110	148	177	196	205	202	189	166	134	93.8	50.9	15.1	0.50	0	0	0
M	0	0	0	0	6.64	31.6	70.2	113	152	185	210	225	232	229	217	196	167	131	90.8	50.3	17.9	1.68	0	0
Jn	0	0	0	0	17.7	47.6	86.1	127	163	194	217	232	238	236	226	208	181	148	110	71.2	35.7	11.2	0	0
Jl	0	0	0	0	9.48	33.8	69.8	110	147	179	202	218	226	224	215	197	171	138	101	62.4	28.7	6.89	0	0
A	0	0	0	0	0	7.96	35.0	73.6	113	148	175	192	200	198	188	168	139	103	64.3	28.3	5.61	0	0	0
S	0	0	0	0	0	0	4.83	30.4	67.9	104	133	152	159	156	142	118	85.3	48.2	15.6	1.10	0	0	0	0
O	0	0	0	0	0	0	0	2.18	21.2	50.8	78.1	96.2	103	98.0	81.8	56.2	26.6	4.75	0	0	0	0	0	0
N	0	0	0	0	0	0	0	0	0.16	11.0	30.7	46.6	53.0	48.5	34.0	14.6	0.74	0	0	0	0	0	0	0
D	0	0	0	0	0	0	0	0	0	0	11.0	25.2	32.8	30.4	18.8	3.06	0	0	0	0	0	0	0	0

Table 8: Horizontal $t_{ssh} = 0.437$

M/h	0	1	2	3	4	5	6	7	8	9	10	11	12	13	14	15	16	17	18	19	20	21	22	23
J	0	0	0	0	0	0	0	0	0	7.79	66.5	96.6	115	115	95.6	65.7	11.1	0	0	0	0	0	0	0
F	0	0	0	0	0	0	0	0	17.3	84.7	142	188	213	214	192	148	91.1	24.0	0	0	0	0	0	0
M	0	0	0	0	0	0	1.45	45.2	121	196	261	306	329	327	303	256	191	117	41.3	0	0	0	0	0
A	0	0	0	0	0	19.6	84.0	158	239	311	368	405	421	416	391	346	283	208	129	59.5	4.42	0	0	0
M	0	0	0	0	36.2	93.3	165	244	319	382	430	461	473	467	444	403	347	278	202	127	67.2	13.1	0	0
Jn	0	0	0	0	67.3	122	193	269	339	399	444	473	486	482	461	425	373	310	238	164	99.2	54.5	0	0
Jl	0	0	0	0	48.5	96.3	163	237	307	368	414	446	460	457	438	403	352	290	219	148	85.8	39.7	0	0
A	0	0	0	0	0	38.0	98.7	170	244	309	360	394	410	407	385	346	291	224	152	85.5	28.7	0	0	0
S	0	0	0	0	0	0	26.4	90.8	160	228	282	317	332	325	299	253	191	123	56.1	7.72	0	0	0	0
O	0	0	0	0	0	0	0	14.3	74.5	129	179	213	226	216	186	138	84.1	23.4	0	0	0	0	0	0
N	0	0	0	0	0	0	0	0	1.49	50.5	92.6	122	134	125	98.5	63.0	6.15	0	0	0	0	0	0	0
D	0	0	0	0	0	0	0	0	0	0	57.1	83.0	97.0	92.4	71.2	28.2	0	0	0	0	0	0	0	0

Table 9: Horizontal $t_{ssh} = 1$

M/h	0	1	2	3	4	5	6	7	8	9	10	11	12	13	14	15	16	17	18	19	20	21	22	23
J	0	0	0	0	0	0	0	0	0	6.04	66.7	115	144	143	113	65.6	8.9	0	0	0	0	0	0	0
F	0	0	0	0	0	0	0	0	14.9	95.4	186	259	299	301	265	196	106	21.6	0	0	0	0	0	0
M	0	0	0	0	0	0	1.07	46.9	153	273	376	447	482	480	442	368	266	147	41.2	0	0	0	0	0
A	0	0	0	0	0	17.3	95.4	213	341	455	544	601	627	619	580	510	412	293	168	61.3	3.36	0	0	0
M	0	0	0	0	32.4	111	224	350	468	567	641	689	708	699	663	600	512	404	284	165	70.6	10.3	0	0
Jn	0	0	0	0	70.5	157	270	390	500	593	662	708	728	721	689	633	553	454	341	226	122	51.0	0	0
Jl	0	0	0	0	44.5	117	222	339	450	545	617	665	687	683	654	599	521	424	313	200	101	34.8	0	0
A	0	0	0	0	0	35.8	121	233	350	453	533	586	610	605	572	511	426	320	206	101	26.3	0	0	0
S	0	0	0	0	0	0	23.6	107	217	324	410	465	488	478	436	364	268	159	60.3	6.31	0	0	0	0
O	0	0	0	0	0	0	0	12.0	81.0	168	247	301	321	306	258	183	96.7	21.8	0	0	0	0	0	0
N	0	0	0	0	0	0	0	0	1.11	48.5	109	155	174	161	119	62.2	4.77	0	0	0	0	0	0	0
D	0	0	0	0	0	0	0	0	0	0	52.1	93.3	116	108	74.6	21.2	0	0	0	0	0	0	0	0

Table 10: 42° degree tilted surface with $t_{ssh} = 0$

M/h	0	1	2	3	4	5	6	7	8	9	10	11	12	13	14	15	16	17	18	19	20	21	22	23
J	0	0	0	0	0	0	0	0	0	3.42	39.6	68.7	84.4	84.0	67.6	38.4	5.07	0	0	0	0	0	0	0
F	0	0	0	0	0	0	0	0	7.32	52.3	96.2	128	145	146	130	100	57.9	11.1	0	0	0	0	0	0
M	0	0	0	0	0	0	0.05	8.74	47.5	93.3	133	161	175	174	159	130	90.8	45.7	7.08	0	0	0	0	0
A	0	0	0	0	0	0.93	4.7	34.4	76.7	118	152	175	185	182	167	140	103	61.5	21.7	3.21	0.16	0	0	0
M	0	0	0	0	1.72	5.29	13.0	50.7	91.6	129	159	179	188	185	170	144	110	71.3	31.9	6.88	3.67	0.51	0	0
Jn	0	0	0	0	3.87	6.89	15.7	52.5	91.5	127	156	176	185	182	169	146	114	77.1	39.0	8.60	5.77	2.86	0	0
Jl	0	0	0	0	2.59	6.25	11.3	44.9	82.4	118	147	167	177	175	163	141	111	75.2	38.6	8.93	5.60	1.99	0	0
A	0	0	0	0	0	2.23	6.87	34.1	71.2	108	138	159	169	167	154	131	99	62.6	27.1	5.88	1.62	0	0	0
S	0	0	0	0	0	0	1.43	19.8	56.2	94.3	126	148	157	153	137	110	74.5	36.7	7.50	0.36	0	0	0	0
O	0	0	0	0	0	0	0	2.31	28.5	66.7	100	121	129	124	104	73.1	35.5	5.45	0	0	0	0	0	0
N	0	0	0	0	0	0	0	0	0.38	26.0	63.1	87.4	96.7	90.2	68.5	35.2	1.77	0	0	0	0	0	0	0
D	0	0	0	0	0	0	0	0	0	0	45.8	74.9	88.5	84.2	62.6	17.6	0	0	0	0	0	0	0	0

Table 11: 42° degree tilted surface with $t_{ssh} = 0.437$

M/h	0	1	2	3	4	5	6	7	8	9	10	11	12	13	14	15	16	17	18	19	20	21	22	23
J	0	0	0	0	0	0	0	0	0	13.2	132	212	254	253	209	129	19.2	0	0	0	0	0	0	0
F	0	0	0	0	0	0	0	0	27.7	167	287	373	417	419	379	297	182	40.4	0	0	0	0	0	0
M	0	0	0	0	0	0	0.87	39.0	154	278	385	459	496	494	453	377	271	148	34.1	0	0	0	0	0
A	0	0	0	0	0	10.8	35.7	117	233	344	434	495	522	515	474	402	303	191	82.0	28.7	2.62	0	0	0
M	0	0	0	0	19.7	36.8	58.1	162	272	373	453	505	528	519	480	413	322	217	109	40.4	31.6	7.61	0	0
Jn	0	0	0	0	32.4	40.7	64.9	166	271	367	443	495	518	511	477	415	331	232	128	44.8	37.1	29.1	0	0
Jl	0	0	0	0	26.5	38.7	52.7	145	247	341	418	471	496	492	461	402	322	226	127	45.4	36.3	22.4	0	0
A	0	0	0	0	0	20.7	40.5	115	216	314	395	451	477	472	438	376	291	192	95.5	37.2	16.0	0	0	0
S	0	0	0	0	0	0	14.9	76.7	176	280	365	422	446	436	393	320	225	122	37.8	4.53	0	0	0	0
O	0	0	0	0	0	0	0	12.8	101	205	295	353	374	358	306	222	120	24.2	0	0	0	0	0	0
N	0	0	0	0	0	0	0	0	1.80	90.5	196	262	287	270	211	120	7.86	0	0	0	0	0	0	0
D	0	0	0	0	0	0	0	0	0	0	149	229	265	254	195	62.5	0	0	0	0	0	0	0	0

Table 12: 42° degree tilted surface with $t_{ssh} = 1$

M/h	0	1	2	3	4	5	6	7	8	9	10	11	12	13	14	15	16	17	18	19	20	21	22	23
J	0	0	0	0	0	0	0	0	0	19.8	214	355	430	428	349	207	29.1	0	0	0	0	0	0	0
F	0	0	0	0	0	0	0	0	42.0	276	486	633	709	712	643	504	303	62.4	0	0	0	0	0	0
M	0	0	0	0	0	0	0.76	54.4	252	472	654	777	838	834	768	641	459	243	45.9	0	0	0	0	0
A	0	0	0	0	0	10.5	39.9	188	392	584	736	835	878	866	799	680	515	319	124	30.2	2.34	0	0	0
M	0	0	0	0	19.3	42.3	81.1	267	461	633	764	848	883	868	806	697	546	364	174	49.8	33.7	6.95	0	0
Jn	0	0	0	0	34.9	50.1	94.0	275	459	622	747	829	865	855	800	701	561	391	208	58.2	44.0	29.4	0	0
Jl	0	0	0	0	26.8	46.7	72.1	238	416	578	705	790	829	823	773	679	545	381	206	59.6	43.0	22.0	0	0
A	0	0	0	0	0	21.5	49.8	185	364	533	668	759	800	792	737	635	492	322	150	44.5	16.3	0	0	0
S	0	0	0	0	0	0	14.9	115	293	473	619	713	752	735	665	543	379	198	49.8	4.30	0	0	0	0
O	0	0	0	0	0	0	0	16.2	158	344	500	599	635	608	519	374	192	33.8	0	0	0	0	0	0
N	0	0	0	0	0	0	0	0	2.44	143	327	443	487	456	353	192	11.0	0	0	0	0	0	0	0
D	0	0	0	0	0	0	0	0	0	0	244	385	449	429	326	97.9	0	0	0	0	0	0	0	0

Table 13: 90° degree tilted surface with $t_{ssh} = 0$

M/h	0	1	2	3	4	5	6	7	8	9	10	11	12	13	14	15	16	17	18	19	20	21	22	23
J	0	0	0	0	0	0	0	0	0	6.11	60.8	91.7	105	105	90.3	58.8	8.90	0	0	0	0	0	0	0
F	0	0	0	0	0	0	0	0	12.3	73.3	111	129	136	136	130	113	78.7	18.2	0	0	0	0	0	0
M	0	0	0	0	0	0	0.09	10.1	54.6	94.3	119	132	136	136	130	117	92.1	52.9	8.33	0	0	0	0	0
A	0	0	0	0	0	1.29	5.08	17.5	57.4	90.5	112	123	127	126	119	105	79.5	43.9	8.40	3.81	0.27	0	0	0
M	0	0	0	0	2.35	5.52	7.88	11.0	48.9	80.8	102	113	117	116	108	92.1	66.2	30.7	8.73	6.64	4.27	0.82	0	0
Jn	0	0	0	0	4.44	6.67	8.75	10.5	39.2	71.2	92.9	105	110	109	101	85.8	60.8	26.3	9.69	7.89	5.80	3.64	0	0
Jl	0	0	0	0	3.32	6.18	8.68	10.8	37.9	69.2	90.9	104	109	108	101	87.2	64.0	32.0	10.2	8.10	5.66	2.69	0	0
A	0	0	0	0	0	2.70	6.64	12.5	46.3	76.8	98.0	110	115	114	107	93.3	70.3	39.0	8.86	5.87	2.03	0	0	0
S	0	0	0	0	0	0	1.85	18.6	54.3	86.0	107	118	122	120	112	96.3	70.1	35.6	5.50	0.52	0	0	0	0
O	0	0	0	0	0	0	0	3.76	40.0	79.5	105	118	122	119	107	84.6	47.7	8.21	0	0	0	0	0	0
N	0	0	0	0	0	0	0	0	0.71	41.2	85.5	106	113	108	90.6	55.0	3.20	0	0	0	0	0	0	0
D	0	0	0	0	0	0	0	0	0	0	72.7	102	113	110	90.9	31.0	0	0	0	0	0	0	0	0

Table 14: 90° degree tilted surface with $t_{ssh} = 0.437$

M/h	0	1	2	3	4	5	6	7	8	9	10	11	12	13	14	15	16	17	18	19	20	21	22	23
J	0	0	0	0	0	0	0	0	0	22.3	202	296	341	340	292	197	32.1	0	0	0	0	0	0	0
F	0	0	0	0	0	0	0	0	44.9	239	362	440	477	478	444	372	255	64.3	0	0	0	0	0	0
M	0	0	0	0	0	0	1.53	51.7	183	303	396	456	484	482	450	388	296	178	46.7	0	0	0	0	0
A	0	0	0	0	0	17.9	53.0	84.3	190	290	368	418	439	433	400	340	255	152	60.2	44.8	4.57	0	0	0
M	0	0	0	0	32.5	53.2	59.1	66.7	166	259	329	375	393	386	354	296	214	116	59.9	54.7	49.0	13.1	0	0
Jn	0	0	0	0	49.8	55.3	60.5	64.7	139	229	299	344	364	358	329	275	198	104	61.7	57.2	52.1	46.9	0	0
Jl	0	0	0	0	42.8	53.6	59.8	65.0	135	223	292	338	359	356	330	279	207	118	62.5	57.2	51.2	36.8	0	0
A	0	0	0	0	0	32.7	55.0	69.6	158	246	317	363	384	381	353	300	226	137	59.4	52.0	25.5	0	0	0
S	0	0	0	0	0	0	24.1	85.9	181	275	349	396	415	406	372	310	226	129	44.2	7.62	0	0	0	0
O	0	0	0	0	0	0	0	20.8	142	256	342	392	410	397	351	272	163	36.9	0	0	0	0	0	0
N	0	0	0	0	0	0	0	0	3.11	141	275	345	370	352	291	184	13.4	0	0	0	0	0	0	0
D	0	0	0	0	0	0	0	0	0	0	235	330	369	357	292	105.4	0	0	0	0	0	0	0	0

Table 15: 90° degree tilted surface with $t_{ssh} = 1$

M/h	0	1	2	3	4	5	6	7	8	9	10	11	12	13	14	15	16	17	18	19	20	21	22	23
J	0	0	0	0	0	0	0	0	0	28.4	291	461	545	543	454	282	41.4	0	0	0	0	0	0	0
F	0	0	0	0	0	0	0	0	57.3	357	583	727	797	799	736	601	387	84.8	0	0	0	0	0	0
M	0	0	0	0	0	0	0.47	46.7	258	475	646	757	811	807	748	633	463	249	38.8	0	0	0	0	0
A	0	0	0	0	0	6.64	25.1	81.0	272	454	596	688	728	717	657	546	391	205	39.8	19.1	1.47	0	0	0
M	0	0	0	0	12.1	27.0	37.5	51.3	230	398	527	610	645	632	572	466	319	142	41.2	31.9	21.4	4.36	0	0
Jn	0	0	0	0	22.1	32.1	41.3	49.0	182	345	472	555	591	582	528	430	290	121	45.5	37.4	28.1	18.6	0	0
Jl	0	0	0	0	16.9	29.9	41.0	50.4	176	335	460	545	584	579	530	438	307	148	47.8	38.3	27.5	13.9	0	0
A	0	0	0	0	0	13.6	31.9	58.1	217	377	505	590	630	623	572	476	341	181	41.7	28.4	10.3	0	0	0
S	0	0	0	0	0	0	9.44	86.0	257	428	563	649	685	669	605	493	339	165	26.4	2.71	0	0	0	0
O	0	0	0	0	0	0	0	17.5	187	391	548	642	675	650	566	421	225	37.9	0	0	0	0	0	0
N	0	0	0	0	0	0	0	0	3.26	194	425	553	598	566	454	260	14.8	0	0	0	0	0	0	0
D	0	0	0	0	0	0	0	0	0	0	352	524	597	575	454	146	0	0	0	0	0	0	0	0